DOT/FAA/AR-06/47

Air Traffic Organization
Operations Planning
Office of Aviation Research
and Development
Washington, DC 20591

Development of a Component Head Injury Criteria (HIC) Tester for Aircraft Seat Certification—Phase 2

January 2007

Final Report

This document is available to the U.S. public through the National Technical Information Service (NTIS), Springfield, Virginia 22161.

U.S. Department of Transportation
Federal Aviation Administration

NOTICE

This document is disseminated under the sponsorship of the U.S. Department of Transportation in the interest of information exchange. The United States Government assumes no liability for the contents or use thereof. The United States Government does not endorse products or manufacturers. Trade or manufacturer's names appear herein solely because they are considered essential to the objective of this report. This document does not constitute FAA certification policy. Consult your local FAA aircraft certification office as to its use.

This report is available at the Federal Aviation Administration William J. Hughes Technical Center's Full-Text Technical Reports page: actlibrary.tc.faa.gov in Adobe Acrobat portable document format (PDF).

Technical Report Documentation Page

1. Report No.	2. Government Accession No.	3. Recipient's Catalog No.
DOT/FAA/AR-06/47		

4. Title and Subtitle	5. Report Date
DEVELOPMENT OF A COMPONENT HEAD INJURY CRITERIA (HIC) TESTER FOR AIRCRAFT SEAT CERTIFICATION—PHASE 2	January 2007
	6. Performing Organization Code
7. Author(s)	8. Performing Organization Report No.
Hamid M. Lankarani	
9. Performing Organization Name and Address	10. Work Unit No. (TRAIS)
National Institute for Aviation Research Wichita State University 1845 N Fairmount Wichita, KS 67260-0093	11. Contract or Grant No. 01-C-AW-WSU Amendment No. 013
12. Sponsoring Agency Name and Address	13. Type of Report and Period Covered
U.S. Department of Transportation Federal Aviation Administration Air Traffic Organization Operations Planning Office of Aviation Research and Development Washington, DC 20591	Final Report
	14. Sponsoring Agency Code
	ANM-100

15. Supplementary Notes

The Federal Aviation Administration Airport and Aircraft Safety R&D Division Program Manager was Gary Frings and the Technical Monitor was Allan Abramowitz.

16. Abstract

The certification of an aircraft interior requires that a head strike to any of the several cabin furnishings comply with the Head Injury Criteria (HIC). This compliance poses a significant problem for many segments of the aerospace industry due to the costs and time required during the development and certification process of 16-g airline seats. The current method of certification requires conducting a full-scale sled test (FSST), which might require the use of a new seat for each dynamic test. It is desirable to use a cheaper, faster, and more repeatable alternative for the certification process. This research addressed the design modification and evaluation of such a device, called the National Institute for Aviation Research Head Injury Component Tester (NHCT).

The performance of the NHCT was evaluated for various aircraft interior surfaces to draw a correlation between FSST and NHCT test results. It was shown that the NHCT was capable of producing conservative HIC results. The performance of the NHCT also was evaluated using analytical models that were developed using the Mathematical Dynamic Model biodynamic occupant simulation code. Analytical models demonstrated that the dynamic response of the NHCT was sensitive to the input parameters.

The NHCT device aim was to provide an alternate means of compliance with the HIC requirement without consuming a seat or seats during certification testing. Preliminary indications showed that modifying the neck of the NHCT from a rigid design to a flexible design improved the performance.

17. Key Words	18. Distribution Statement
Head Injury Criteria (HIC), Component tester, MADYMO, Aircraft seat test, Simulation	This document is available to the public through the National Technical Information Service (NTIS) Springfield, Virginia 22161.

19. Security Classif. (of this report)	20. Security Classif. (of this page)	21. No. of Pages	22. Price
Unclassified	Unclassified	55	

Form DOT F1700.7 (8-72) Reproduction of completed page authorize

ACKNOWLEDGMENTS

The authors gratefully acknowledge the contribution of the staff at the Federal Aviation Administration Civil Aerospace Medical Institute for conducting a series of tests at their facility to evaluate the performance and assist with the setup of the Head Injury Criteria Component Tester Device. Special thanks go to Mr. Van Gowdy, Mr. Richard L. DeWeese, and Mr. David M. Moorcroft.

TABLE OF CONTENTS

		Page
EXECUTIVE SUMMARY		xiii
1.	INTRODUCTION	1
2.	BACKGROUND	1
3.	DESCRIPTION OF NHCT	2
4.	MODIFICATION OF THE NHCT	5
5.	PRELIMINARY EVALUATION OF THE NHCT AT NIAR	7
5.1	Baseline FSSTs Using Aluminum Panels	8
5.2	Comparable NHCT Tests Using Aluminum Panels	9
5.3	Comparison of NHCT Results With FSST Results	11
5.3.1	Evaluation of NHCT Tests 01057-71 and 01057-72 With FSST 96288-16 (Aluminum Panel)	11
5.3.2	Evaluation of NHCT Test 01057-49 Compared With FSST 01008-008 (Nomex Honeycomb Panel)	13
6.	MODELING AND ANALYSIS OF NHCT AND FSST USING MADYMO	14
6.1	Setup of the MADYMO Model for the NHCT	14
6.2	MADYMO Model Setup for the FSST	16
6.3	Parametric Study of Impact Surface Stiffness and Setback Distances	19
6.3.1	Parametric Study With FSST	19
6.3.2	Parametric Study With NHCT	21
6.4	Correlation of MADYMO Models for FSST and NHCT	22
6.4.1	Panel Stiffness and HIC at an Impact Angle of 31 Degrees	22
6.4.2	Panel Stiffness and HIC at an Impact Angle of 40 Degrees	23
6.4.3	Panel Stiffness and HIC at an Impact Angle of 53 Degrees	24
6.4.4	Correlation of FSST and NHCT HIC Models	25
7.	SUMMARY OF CAMI NHCT TESTS	26
8.	EVALUATION OF NHCT TESTS CONDUCTED AT CAMI	28

8.1 Raw Test Data 29
8.2 Validated MADYMO NHCT and FSST Models 30

8.2.1 Validation of FSST MADYMO Model 30
8.2.2 Validation of NHCT MADYMO Model 34

8.3 Use of MADYMO NHCT Model to Obtain HIC Values for Input Parameters Matched to FSSTs 36

8.4 Correlation Between FSST Results and MADYMO NHCT Results 37

9. EVALUATION OF NHCT WITH A FLEXIBLE NECK 38

10. RESULTS 41

11. REFERENCES 42

LIST OF FIGURES

Figure		Page
1	Design of NHCT	3
2	Fabricated NHCT	3
3	Design Methodology for the NHCT	4
4	Comparison of Pertinent Parameters for FSST and NHCT	4
5	Computer Block Diagram and Control Screens	5
6	Electronic Pressure Regulator	6
7	Solenoid Supply Valve and Bursting Disc	6
8	Pressure Sensor	7
9	Computer Screen With Posttest Data	7
10	Acceleration Plots for FSST 96288-16	8
11	Velocity Plots for FSST 96288-16	8
12	Data Plots for NHCT Test 01057-72	10
13	Evaluation of Resultant Acceleration for NHCT Tests 01057-71 and 72 With FSST 96288-16	12
14	Repeatability of NHCT Tests 01057-71 and 72	12
15	Comparison of NHCT Test 01057-49 With FSST 01008-8 for Head c.g. Resultant Acceleration	13
16	Process Flow for FSST-NHCT Parametric Study	14
17	Setup of the MADYMO Model for Test 01057-82	15
18	Load Displacement for Panel Used for Test 01057-82	15
19	Head Acceleration Profiles for MADYMO Model and NHCT Test 01057-82	16
20	MADYMO Model Setup for FSST 97191-003	17
21	Load Displacement for Slitted Panel	17
22	Load Displacement for MADYMO Belt Used	17

23	Input Pulse for FSST MADYMO Model	18
24	Head Acceleration Profile for MADYMO Model and FSST 9719-003	18
25	Setup of the MADYMO With ETHAFOAM Panel	19
26	Linear Load Deflection Properties of the ETHAFOAM Panel	19
27	MADYMO Simulation Input Pulse	20
28	MADYMO Lap Belt Load Deflection Properties	20
29	Seat Cushion Load Deflection Properties	20
30	Simulation of the FSST With ETHAFOAM Panel	21
31	Simulation Sequence for Impact Angle of 53 Degrees With ETHAFOAM Panel for the NHCT	22
32	The HIC Correlation for FSST and NHCT MADYMO Models With an Impact Angle of 31 Degrees	23
33	The HIC Correlation for FSST and NHCT MADYMO Models With an Impact Angle of 40 Degrees	24
34	The HIC Correlation for FSST and NHCT MADYMO Models With an Impact Angle of 53 Degrees	24
35	Comparison of MADYMO Models of HIC-FSST vs HIC-NHCT for 31-, 40-, and 53-Degree Impact Angles (Seat Setback of 28, 32, and 37 Inches)	25
36	Different Impact Surfaces Used for CAMI Tests	26
37	Process Flow for Analytical-Experimental Model	28
38	ETHAFOAM Setup for FSST A03007	29
39	Corresponding NHCT Test for FSST A03007	29
40	Finite Element Model of Polyethylene Foam Pad With Duct Tape (Straps)	30
41	MADYMO Model Developed for FSST	31
42	Acceleration Pulse for FSST A03007	31
43	Foam Load Deflection Properties	32
44	Simulation Sequence for Head Strike for FSST A03007	32

45	Simulation Sequence of Foam Deformation and its Relative Motion With Rigid Surface for FSST A03007	33
46	Head Acceleration for FSST and MADYMO Model	33
47	Simulation Sequence for Head Strike NHCT Test H03316	34
48	Simulation Sequence of Foam Deformation and its Relative Motion With Rigid Surface for NHCT Test H03316	35
49	Head Acceleration Profile for Actual Test and Simulation	35
50	Correlation of MADYMO NHCT and FSST	37
51	Head Rotation Angle and Impact Angle	38
52	Head Rotation for Impact Angle of 40 Degrees	38
53	Head Impact for Sled Test and NHCT With Flexible Neck on Polyethylene Pad	39
54	Simulation Sequence for NHCT With Flexible Neck	39
55	Comparison of Head Acceleration Profile for FSST and NHCT Model With Flexible Neck	40
56	Correlation Between FSST and NHCT With Rigid and Flexible Necks	41

LIST OF TABLES

Table		Page
1	Test Results of FSST 96288-16	9
2	Test Results of FSSTs 96288-04 to 96288-23	9
3	Test Results of NHCT Tests 01057-55 to 01057-106	10
4	Comparison of NHCT 01057-71 and 72 With FSST 6288-16	12
5	Comparison of NHCT Test 01057-49 With FSST Test 01008-008 (Nomex Honeycomb Panel)	13
6	Comparison of NHCT Test 01057-82 With MADYMO Simulation	16
7	Comparison of FSST 97191-003 With MADYMO Simulation	18
8	The FSST Simulation Results of Panel Stiffness and Impact Angles	21
9	Simulation Results of Panel Stiffness and Impact Angle for the NHCT	22
10	Results of the FSST and NHCT Test Using Different Impact Surfaces	27
11	FSST and NHCT Tests With ETHAFOAM Impact Surface	30
12	Comparison of FSST A03007 With MADYMO Simulation	34
13	Comparison of NHCT Test H03316 With MADYMO Simulation	36
14	Comparison of HIC Results for FSST and NHCT	36
15	Comparison of HIC Results for FSST and MADYMO NHCT	37
16	Comparison of Flexible and Rigid Neck NHCT Model Results and Corresponding FSST Results	40
17	Comparison of FSST Results With Flexible Neck NHCT Model Results	41

LIST OF SYMBOLS AND ACRONYMS

ATD	Anthropomorphic test dummy
c.g.	Center of gravity
CAMI	Civil Aerospace Medical Institute
CFR	Code of Federal Regulations
EPR	Electronic pressure regulator
FAA	Federal Aviation Administration
FE	Finite element
FSST	Full-scale sled test
HIC	Head Injury Criteria
MADYMO	Mathematical Dynamic Model
NHCT	National Institute for Aviation Research Head Injury Component Tester
NIAR	National Institute for Aviation Research

EXECUTIVE SUMMARY

Compliance with the Head Injury Criteria (HIC) requirement represents a significant challenge to engineers designing cabin interior furnishings for all classes of aircraft. The Federal Aviation Administration certification of aircraft interiors requires compliance with the HIC requirement as specified in Title 14 Code of Federal Regulations Parts 23.562 and 25.562. Full-scale sled tests (FSST), which are extensively used to evaluate the design of interior furnishings, are destructive tests that might consume several test articles in demonstrating design compliance. HIC compliance poses a significant problem for the airlines and manufacturers due to the costs and time required during the development and certification of 16-g airline seats. These factors have led to the development and potential applicability of a device that will evaluate a design without consuming a seat.

The National Institute for Aviation Research (NIAR) Head Injury Criteria Component Tester (NHCT) was designed and fabricated based on a series of FSSTs conducted at NIAR. This device aimed to duplicate full-scale results and operated in a manner that reproduced the forces and accelerations generated in a full-scale test. The NHCT can produce similar inertial system forces that create the same impact velocities and acceleration profiles observed in full-scale tests. Validation of the NHCT was conducted in this study using the biodynamic occupant simulation code Mathematical Dynamic Model (MADYMO) and data from FSSTs. HIC results were compared to FSST results for resultant-head acceleration, HIC, HIC window size, head-impact angle, head-impact velocity, and average head center of gravity acceleration values.

Performance of the NHCT was evaluated for various aircraft interior surfaces and compared to results from the FSST. The NHCT produced conservative HIC results compared to the FSSTs. HIC for the HHCT was evaluated for front-row bulkhead seating and row-to-row seating using MADYMO.

It was observed that the dynamic response of the NHCT was very sensitive to input parameters. Preliminary indications showed that modifying the neck of the NHCT from a rigid design to a flexible design resulted in decreased differences between the NHCT and FSST results.

1. INTRODUCTION.

One of the problems encountered in the certification of 16-g airline seats is what is referred to as the front-row Head Injury Criteria (HIC) problem. This problem occurs for seats located directly behind bulkheads or cabin class dividers. These structures are typically both stiff and strong and tend to produce very high HIC values during head impacts. Another HIC-related issue was encountered in the certification of seats located behind other seats that incorporate devices (such as drop-down tables) and other hard structures (such as video displays). This problem is referred to as the row-to-row HIC problem. Currently, several full-scale sled tests (FSST) are required to determine the HIC values that are produced during head impacts with these bulkheads or front seat structures. Normally, seats used for these tests are destroyed, consequently resulting in significant costs.

The objective of this research project is to evaluate a component test apparatus that aims to effectively support the design and certification of aircraft seats to meet HIC requirements. This device will minimize the need for full-scale tests and reduce the associated time and cost for development and certification .

2. BACKGROUND.

Chandler [1] described the development of the HIC that evolved from the Wayne State Tolerance Curve [2]. Gadd [3] defined the severity index based on raising the time integral of head acceleration in g's to the power of 2.5, after observing this to be the slope of the line that closely fit the Wayne State data when it was plotted using a log-log scale. Gadd also proposed the injury threshold of 1000. Versace [4] subsequently advocated the use of an effective acceleration, which he defined as

$$\{ {}^{1}\!/_{t} \int a^{2.5}\, dt \},$$

where t and a, respectively, represent the time interval and resultant head acceleration. The HIC was subsequently defined by Gurdjian [5 and 6] as

$$\text{HIC} = \left[(t_2 - t_1) \left\{ \frac{1}{(t_2 - t_1)} \int_{t_1}^{t_2} a(t)dt \right\}^{2.5} \right]_{\max}$$

where:

$a(t)$ = resultant acceleration of the head center of gravity (c.g.) in g's
t_1 = initial integration time, expressed in seconds
t_2 = final integration time, expressed in seconds

Maximization is performed by identifying the time interval $t_2 - t_1$ that results in the largest functional value. This criterion was adapted from the Federal Motor Vehicle Safety Standard No. 208 [7]. In aerospace applications, the definition differs in that the HIC is evaluated over the period when the head of the anthropomorphic test dummy (ATD) is in contact with any structure on the aircraft interior. Injury is defined as any HIC value exceeding the threshold value of 1000. The HIC subsequently was recommended as one of the injury criteria by the General

Aviation Safety Panel to be considered in the design and certification of aircraft seats and restraint systems. HIC requirements were adapted and are specified in Title 14 Code of Federal Regulations (CFR) Parts 23.562 [8] and 25.562 [9].

Alternative methods involving the use of component test devices represent useful engineering tools for HIC evaluation in both the aircraft and the automotive industries. A validated component test device should be simple to use, operate, and control. The device should show good repeatability and produce less data scatter than that obtained from a FSST. Validation of an HIC component tester requires that the measurements of the following parameters from component tests agree with the values of corresponding parameters acquired from FSSTs.

- HIC
- Average head c.g. resultant acceleration and duration
- HIC window, $\Delta t = t_2 - t_1$
- Head c.g. resultant acceleration profile

Component testers include the following:

- Bowling Ball Tester
- Free Motion Headform Tester
- MGA Head/Neck Impactor
- Pendulum Test Rig Tester

A study of these devices determined that they do not provide adequate correlation with the FSSTs for required test conditions [10]. The component-level devices provide reasonable correlation compared with the 16-g dynamic FSSTs only for configurations with predominantly normal head impact velocities, short distances from the impact surface, and relatively short-duration impacts. Factors affecting these differences may include articulation of other body segments for the ATD, belt compliance, translation motion of the pelvis, and friction of the pelvic/seat and head/frontal structure. The National Institute for Aviation Research (NIAR) has developed an HIC component tester designed to overcome the problems facing existing component testers and reproduce the test results of FSSTs of a Hybrid II ATD (49 CFR Part 572).

3. DESCRIPTION OF NHCT.

The National Institute for Aviation Research Head Injury Criteria Component Tester (NHCT) was designed to mimic the kinematics of a 50th percentile male Hybrid II ATD during dynamic testing. The device was intended to produce the same HIC and other kinematics values as a FSST. The following section briefly discusses the design and development of the NHCT.

The NHCT device, shown in figures 1 and 2, consists of a Hybrid II ATD head mounted on an aluminum pendulum arm (collectively the upper torso) attached to a translating aluminum mass representing the lower torso. The pendulum arm weighs 7 lb, is 21.2 inches long, and is pinned to the lower torso so that the pendulum can pivot. The mass distribution of the tester is different from the ATD that has variable inertia compared to the ATD due its flailing limbs. This mass

distribution was obtained by optimizing the system response for the head acceleration equivalence. The Hybrid II ATD head is connected to the pendulum arm through the neck bracket. Unlike the ATD that has a rubber neck, the NHCT neck is fabricated from rigid polycarbonate. An actuator propels the pendulum through a pivoting support arm and the attached support arm extension. The actuator is mounted on a stand and is supported by bearings on either ends of the trunion. The stand assembly and support arm are bolted in place. The lower torso is attached to two sets of linear bearings that slide on the rails, allowing it to translate forward and aft. This translation represents the ATD snap back in an FSST.

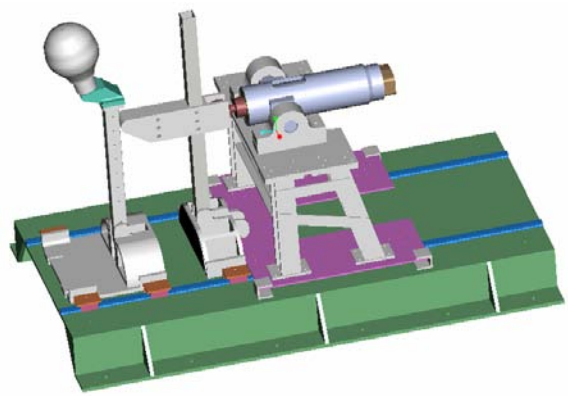

Figure 1. Design of NHCT

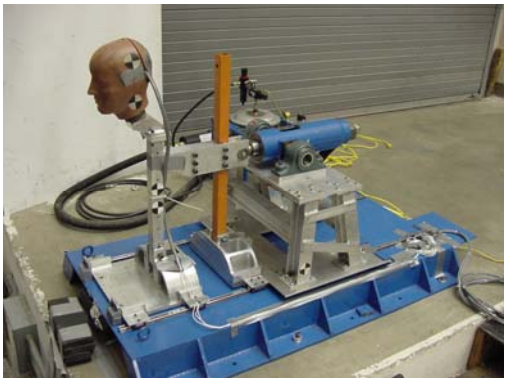

Figure 2. Fabricated NHCT

The propulsion system consists of a bottle of pressurized nitrogen gas, an accumulator, a gas valve, tubing, and a control system. Pressurized nitrogen gas is used to charge the accumulator to the required pressure. The accumulator, when triggered by the control system, discharges the nitrogen gas into the actuator, driving the pendulum arm forward.

Development of this device as described has followed an iterative approach, which is outlined in figure 3. The methodology included analyzing FSST data, modeling the ATD kinematics through biodynamic simulations, creating a biodynamic model of the tester, conducting a parametric study of the design, designing and fabricating the tester, and finally performing a preliminary evaluation of the tester.

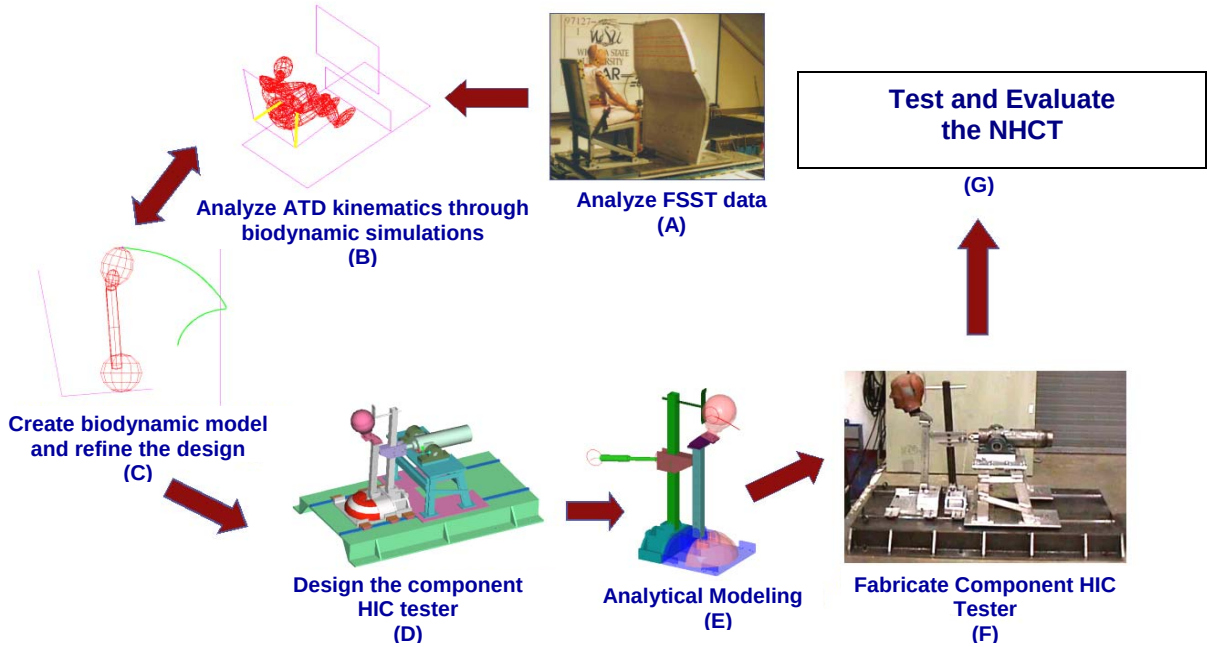

Figure 3. Design Methodology for the NHCT

The test conditions for the NHCT were set to mimic the geometry and the dynamics of the FSST. Some of the parameters taken into account are shown in figure 4. The arm of the NHCT, which is the analogue of the ATD's torso, is designed to rotate around a pivot that corresponds to the H point on the ATD. The length of the NHCT arm and the length of the ATD torso are of a similar ratio. Likewise, the setback distance (distance between the intersection point of the seat cushion and seat back to the frontal structure/bulkhead) of the NHCT pivot point from the impact location is similar, corresponding to the distance between the edge point and the impact surface of the associated FSST.

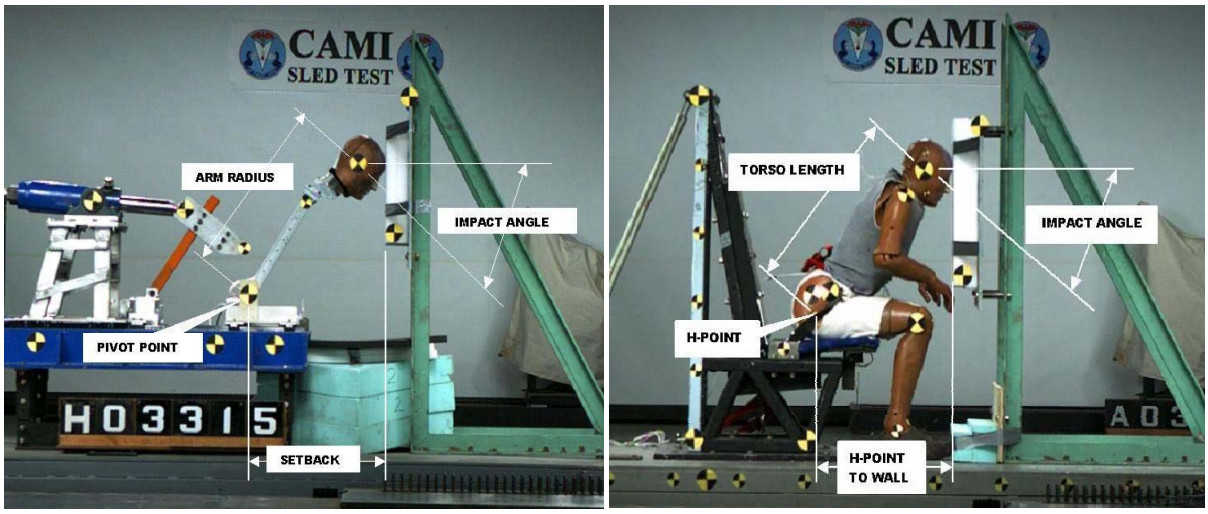

Figure 4. Comparison of Pertinent Parameters for FSST and NHCT

4. MODIFICATION OF THE NHCT.

Since HIC values generated by the device are a direct function of the accumulator pressure, lack of repeatability in actuator pressure directly affects the device's ability to produce repeatable results. The initial design used a manual means to ensure appropriate pretest nitrogen pressure in the accumulator. Safety issues aside, this arrangement also resulted in significant variations in accumulator pressure from test to test. The problems were resolved by placing the device under the control of a computer that, among other functions, was able to control an electronic pressure regulator (EPR). This resulted in repeatable accumulator nitrogen pressures. The interface computer also automated many of the functions that previously had been performed manually. A block diagram of this computer is shown in figure 5.

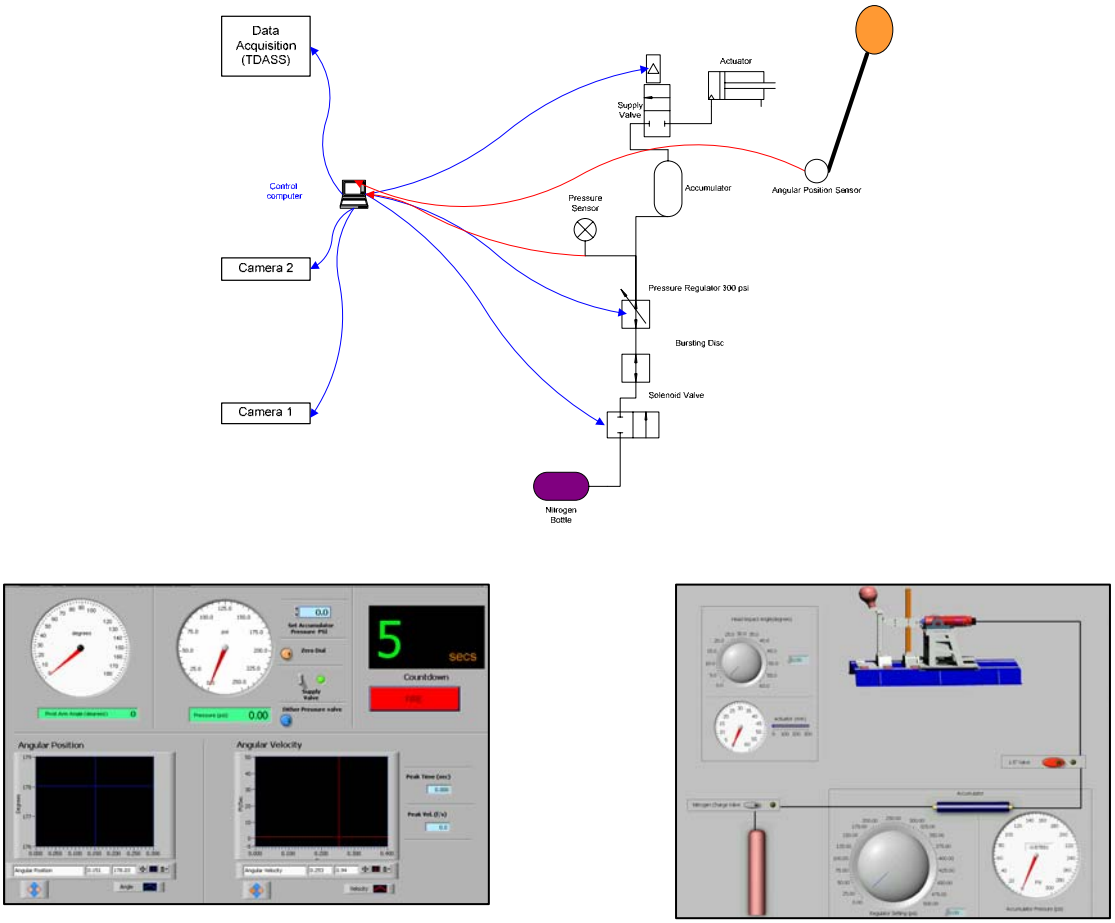

Figure 5. Computer Block Diagram and Control Screens

As may be noted from the block diagram, the computer can handle most operations required to operate the device, including opening the gas supply valve, triggering the actuator, and acquiring data.

During operation, the desired operating pressure is set, the supply valve is opened, and the accumulator is pressurized to the desired pressure by the interface controller via the EPR shown

in figure 6. The regulator is a card-mounted device that does not require gas flow to maintain pressure. This design eliminates the discharge of vented nitrogen while maintaining constant pressure in the accumulator, thus ensuring that no nitrogen is lost during the process. The low, minimum-control volume of 1 in^3 ensures a smooth buildup of pressure and allows fine adjustments to be made.

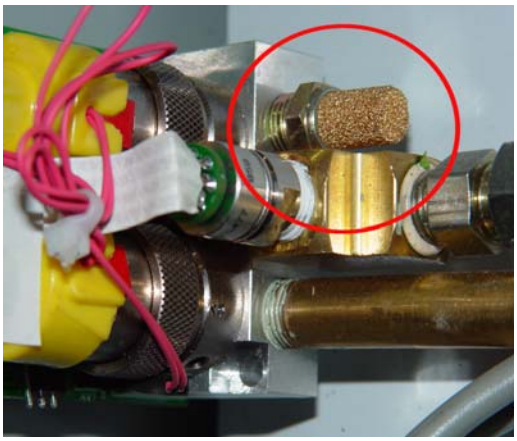

Figure 6. Electronic Pressure Regulator

A silencer was added to the EPR primarily to prevent dust from entering the solenoid spool. A bursting disc (figure 7) was included upstream of the solenoid valve to protect the low-pressure components of the gas supply system from the high-side (gas bottle) pressure of up to 3000 psi.

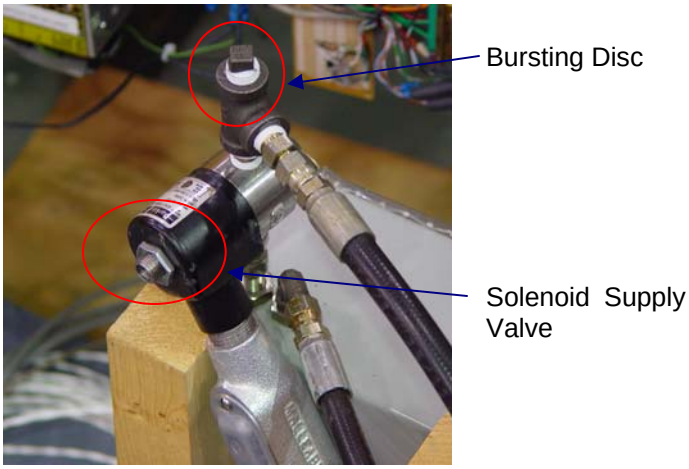

Figure 7. Solenoid Supply Valve and Bursting Disc

The accumulator was instrumented with a pressure sensor (figure 8) that provided the computer with a feedback loop created using the pressure sensor, computer, and the EPR to obtain repeatable accumulator pressures.

Figure 8. Pressure Sensor

Once the accumulator is filled to the desired pressure, the system is ready to be activated via the computer. Doing so initiates a 5-second countdown and automatic triggering of the camera and data acquisition system. The system then triggers the solid-state relays, which open the main supply valve from the accumulator to the actuator, thus driving the pendulum arm into the test article. A sensor mounted on the pendulum arm base measures angular position from which the computer calculates both peak velocity and peak time (figure 9).

Figure 9. Computer Screen With Posttest Data

5. PRELIMINARY EVALUATION OF THE NHCT AT NIAR.

A preliminary evaluation of the NHCT was conducted at NIAR [11]. The NHCT had been previously calibrated and evaluated for a setback distance of 35 inches. Although this is the most common seating configuration, other distances related to various cabin class configurations

needed to be studied. For this, baseline FSSTs as well as component tests were conducted for other seat setback distances using aluminum and Nomex panels and bulkheads. The tester produced reasonably good performance in replicating the results of the FSSTs for the range of seat setback distances tested, especially for small seat setback angles.

5.1 BASELINE FSSTs USING ALUMINUM PANELS.

A series of 12 FSSTs were conducted using a 0.063-inch-thick aluminum panel (Al 2024-T3) as the bulkhead. The seat setback distance was varied from 28 to 35 in. to obtain head impact angles from 27 to 61 degrees. The details of the tests and the results are discussed below.

A polyester lap belt was used for restraining the Hybrid II ATD. A load cell was attached to the lap belt to determine the belt forces. Figures 10 and 11 show the FSST data plots obtained from test 96288-16, the seat setback distance was 33.5 in. The results are listed in table 1.

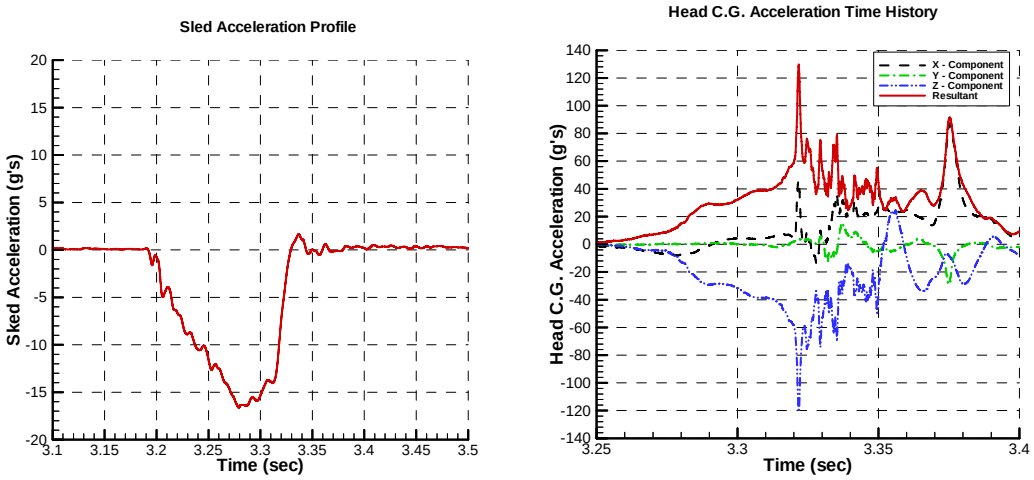

Figure 10. Acceleration Plots for FSST 96288-16

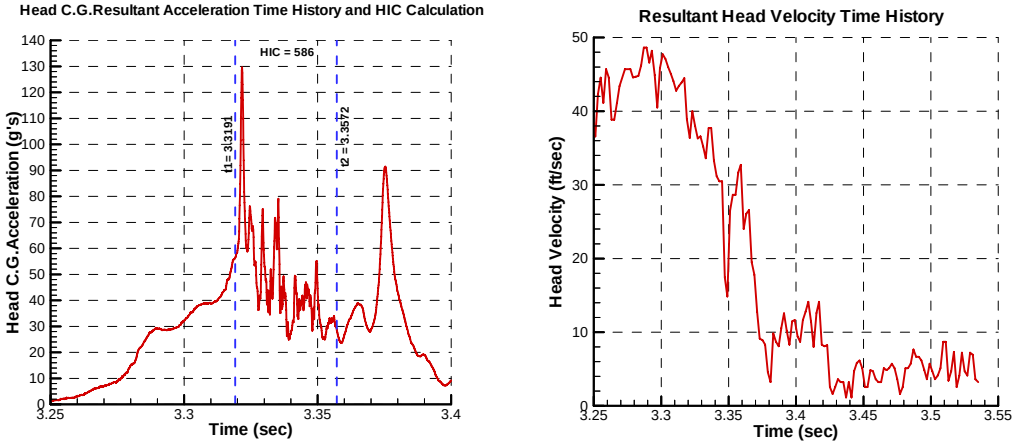

Figure 11. Velocity Plots for FSST 96288-16

Table 1. Test Results of FSST 96288-16

Parameter	FSST 96288-16
Seat setback distance (in.)	33.0
Head impact angle (deg)	44.0
Head impact velocity (ft/sec)	38.9
Sled peak deceleration (g's)	16.6
HIC	586.0
HIC window (ms)	38.1
Head c.g. resultant peak acceleration (g's)	129.6
Head c.g. resultant average acceleration (g's)	47.4

Similarly, results from other FSSTs conducted for different head impact angles are listed in table 2.

Table 2. Test Results of FSSTs 96288-04 to 96288-23

Test No.	Seat Setback Distance (in.)	Head Impact Velocity (ft/sec)	Head Impact Angle (deg)	Head c.g. Acceleration (g's)		HIC	HIC Window (sec)
96288-14	35	41.7	61	153.4	47.2	361	23.8
96288-15	34	41.6	51	215.6	180.4	777	1.9
96288-16	33.5	38.9	44	129.6	47.4	586	38.1
96288-17	34.5	42.9	56	113.9	49.6	549	31.9
96288-18	30.6	45.0	38	209.0	64.6	924	27.5
96288-19	28.6	43.6	28	205.4	78.0	1193	22.3
96288-20	29.6	44.4	31	175.3	69.0	906	23.0
96288-22	33.5	52.7	48	143.6	49.5	716	41.8

5.2 COMPARABLE NHCT TESTS USING ALUMINUM PANELS.

Corresponding to the FSSTs, a series of NHCT tests were conducted to evaluate the performance of the NHCT. The NHCT settings were selected to reproduce the FSST impact parameters. The test procedure for the NHCT and data plots for a representative test, 01057-72, are given.

NHCT test 01057-72 was conducted using a 0.063-inch-thick aluminum panel (Al 2024-T3) as the bulkhead. This test corresponded with FSST 96288-016. The panel was positioned such that it resulted in a head impact angle of 44 degrees. The accumulator pressure was set to 150 psi to obtain a head impact velocity of 38.9 ft/sec as calculated from the NHCT calibration charts.

Triaxial accelerometers mounted on the Hybrid II ATD head measured the head accelerations in the x, y, and z directions. A high-speed camera was used to record the NHCT's kinematics. Figure 12 shows the data plots, and table 3 shows the results obtained from the analysis of various tests.

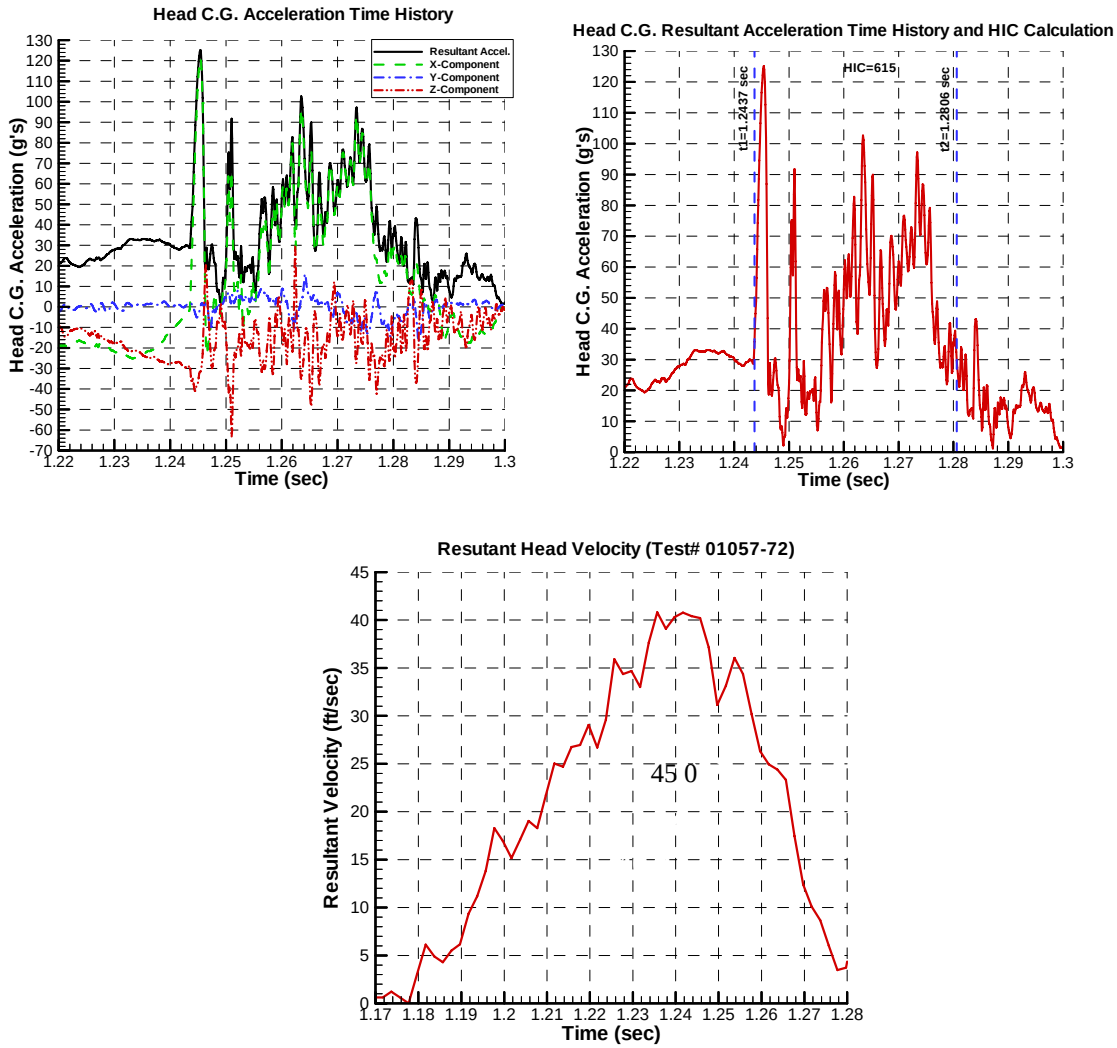

Figure 12. Data Plots for NHCT Test 01057-72

Table 3. Test Results of NHCT Tests 01057-55 to 01057-106

Test No.	Head Impact Velocity (ft/sec)	Head Impact Angle (degree)	HIC Window (ms)	HIC
01057-55	45.0	50	20.0	623
01057-56	46.7	50	36.2	799
01057-57	46.2	53	36.2	766
01057-68	40.0	46	31.9	614
01057-69	40.6	44	35.9	655
01057-70	39.0	43	70.4	620
01057-71	39.5	44	35.2	659
01057-72	40.4	45	36.9	615
01057-73	44.8	59	32.5	183

Table 3. Test Results of NHCT Tests 01057-55 to 01057-106 (Continued)

Test No.	Head Impact Velocity (ft/sec)	Head Impact Angle (degree)	HIC Window (ms)	HIC
01057-74	42.4	60	45.4	208
01057-75	42.4	60	42.6	232
01057-76	41.6	59	43.8	226
01057-82	46.0	40	22.6	1271
01057-84	49.0	49	40.8	797
01057-85	50.6	48	39.4	861
01057-86	51.7	49	41.3	1026
01057-87	51.7	49	41.1	855
01057-88	52.7	48	43.5	993
01057-89	50.3	49	32.5	1227
01057-90	52.7	48	34.4	1360
01057-91	52.0	47	35.1	1449
01057-92	45.3	38	30.9	1184
01057-93	46.7	38	29.1	1695
01057-94	46.2	38	28.8	1711
01057-96	46.3	38	29.4	1310
01057-97	44.7	38	30.5	987
01057-98	44.3	38	28.8	1194
01057-99	36.6	31	31.4	1478
01057-100	44.5	31	31.1	1642
01057-101	44.4	31	29.8	1516
01057-102	45.7	38	30.4	1047
01057-103	44.0	38	34.8	843
01057-104	45.3	38	30.3	601
01057-105	45.4	38	20.2	721
01057-106	44.6	38	30.7	858

5.3 COMPARISON OF NHCT RESULTS WITH FSST RESULTS.

Results of the aluminum panel tests were compared, and good correlation was found between the FSST results and the NHCT results. The data plots and test results for a representative test set from this series are discussed below.

5.3.1 Evaluation of NHCT Tests 01057-71 and 01057-72 With FSST 96288-16 (Aluminum Panel).

A FSST was conducted with a head impact angle of 44 degrees. A 0.063-inch-thick aluminum panel was used for the test. NHCT tests 01057-71 and 72 were conducted using similar setup parameters to check for repeatability. Figure 13 shows the evaluation plots of the resultant acceleration for NHCT tests 01057-71 and 72 with FSST 96288-16.

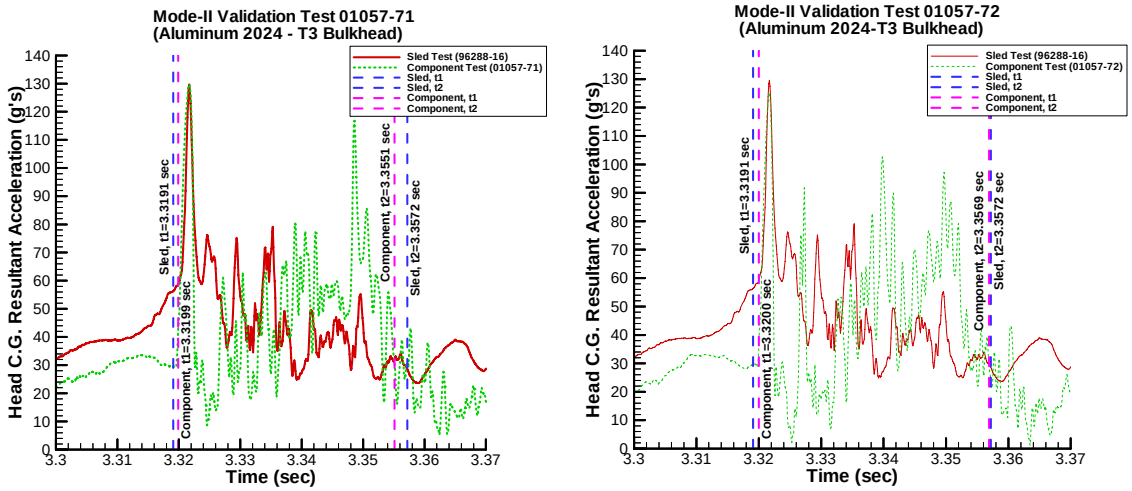

Figure 13. Evaluation of Resultant Acceleration for NHCT Tests 01057-71 and 72 With FSST 96288-16

The repeatability plots of NHCT test 01057-71 and 72 are shown in figure 14. A comparison of NHCT results with an FSST is listed in table 4.

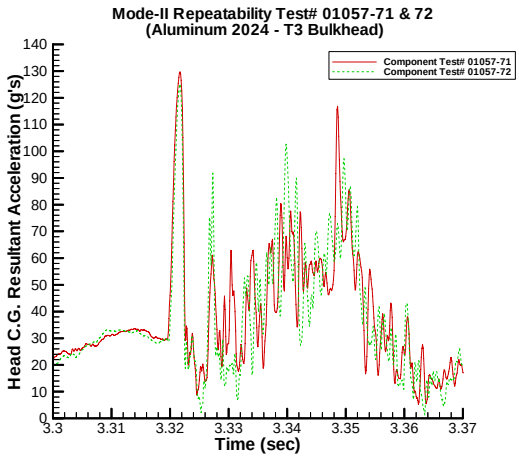

Figure 14. Repeatability of NHCT Tests 01057-71 and 72

Table 4. Comparison of NHCT 01057-71 and 72 With FSST 6288-16

Parameter	FSST 96288-16	NHCT Test 01057-71	NHCT Test 01057-72
Head impact angle (deg)	44.0	44.0	45.0
Head impact velocity (ft/sec)	38.9	39.5	40.4
HIC	586.0	659.0	615.0
HIC window (ms)	38.1	35.2	36.9
Head c.g. peak acceleration (g's)	129.6	129.7	125.2
Head c.g. avg. acceleration (g's)	47.4	51.1	36.9

From the above data plots and the results, it was found that the NHCT results correlated well with the FSST results for peak and duration of the initial contact and had good repeatability.

5.3.2 Evaluation of NHCT Test 01057-49 Compared With FSST 01008-008 (Nomex Honeycomb Panel).

An NHCT test was conducted to compare the data obtained with that from FSST 01008-008. Results are listed in table 5. Figure 15 shows the comparison plots of the head c.g. resultant acceleration profiles of NHCT test 01057-49 and FSST 01008-008.

Table 5. Comparison of NHCT Test 01057-49 With FSST Test 01008-008 (Nomex Honeycomb Panel)

Description	FSST Test 01008-008	NHCT Test 01057-49
HIC	862	800
Head impact angle (deg)	40.0	38.7
Head-impact velocity (ft/sec)	44.5	41.2
HIC window (ms)	28.7	12.1
Head c.g. peak acceleration (g's)	132.3	109.0
Head c.g. avg. acceleration (g's)	61	73

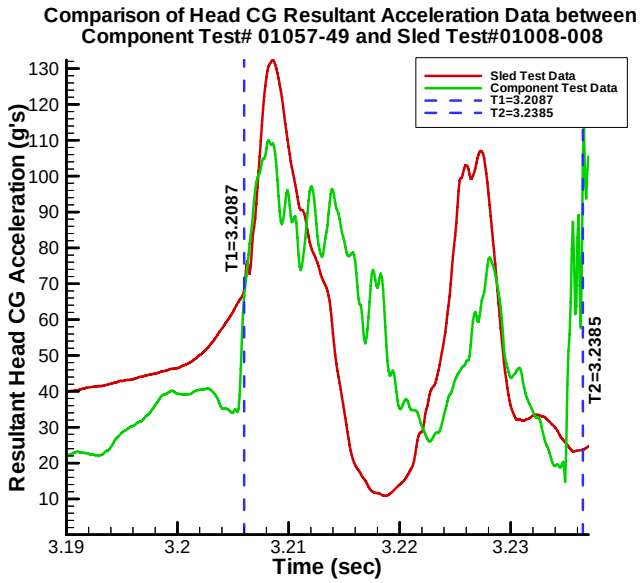

Figure 15. Comparison of NHCT Test 01057-49 With FSST 01008-8 for Head c.g. Resultant Acceleration

Preliminary panel evaluation tests conducted at NIAR indicated that the NHCT generally provided values that underpredict HIC compared to the FSST by as much as 15 to 17 percent.

6. MODELING AND ANALYSIS OF NHCT AND FSST USING MADYMO.

A series of analytical models were built using the biodynamic occupant simulation code Mathematical Dynamic Model (MADYMO) to study the influence of various test parameters and their effects on the FSST and NHCT test results. These models were validated against appropriate FSST and NHCT tests. A flow chart depicting this process is provided in figure 16.

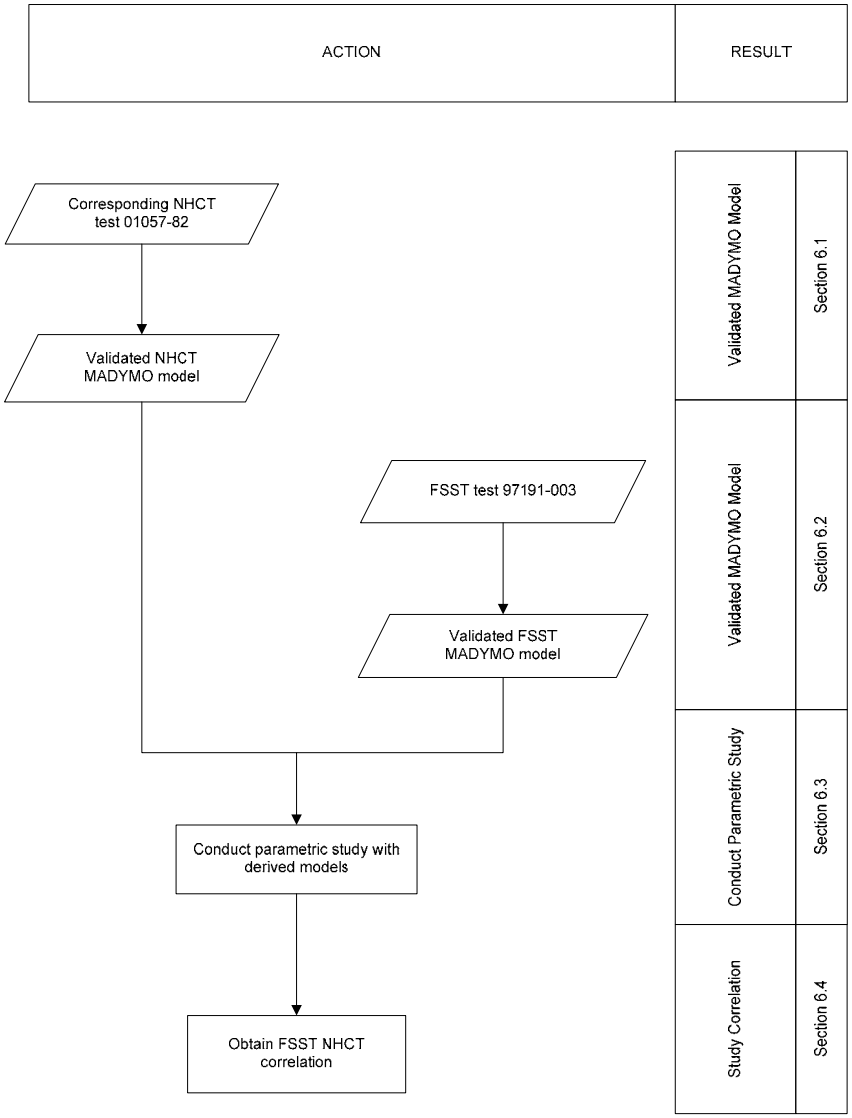

Figure 16. Process Flow for FSST-NHCT Parametric Study

6.1 SETUP OF THE MADYMO MODEL FOR THE NHCT.

The NHCT MADYMO model was built from three bodies: a slider joined to the reference space via a translational joint, a pendulum arm connected to the slider through a revolute joint, and a neckpiece connected to the head with rigid joints. The head used was identical to that of a 50th percentile male Hybrid II ATD.

Test 01057-82 conducted at NIAR was selected for the MADYMO model. A panel with vertical slits 4 inches apart was used in this test. The pivotal setback distance was 23.5 inches, and the operating pressure selected for the desired head impact velocity was 170 psi. A friction coefficient of 0.3 was used between the head and the panel. The point of acceleration sensor attachment is highlighted in the head. Figure 17 shows the actual NHCT test as well as the MADYMO model.

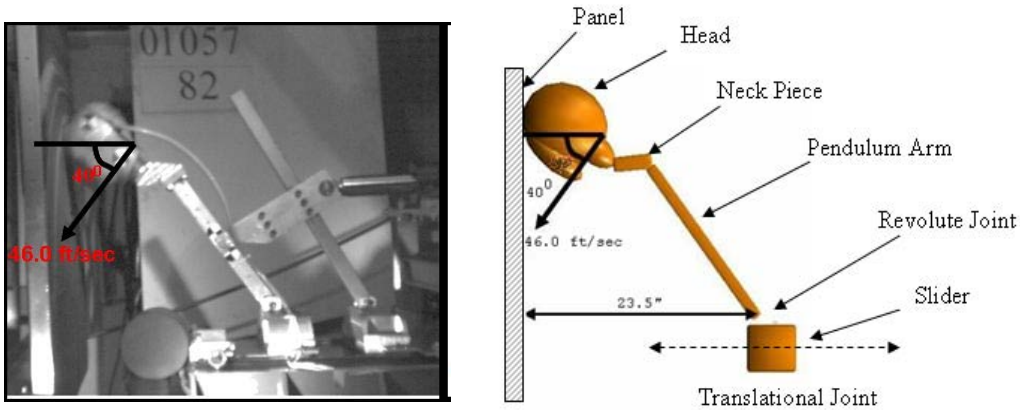

Figure 17. Setup of the MADYMO Model for Test 01057-82

The panel was modeled as a plane with load displacement properties as depicted in figure 18.

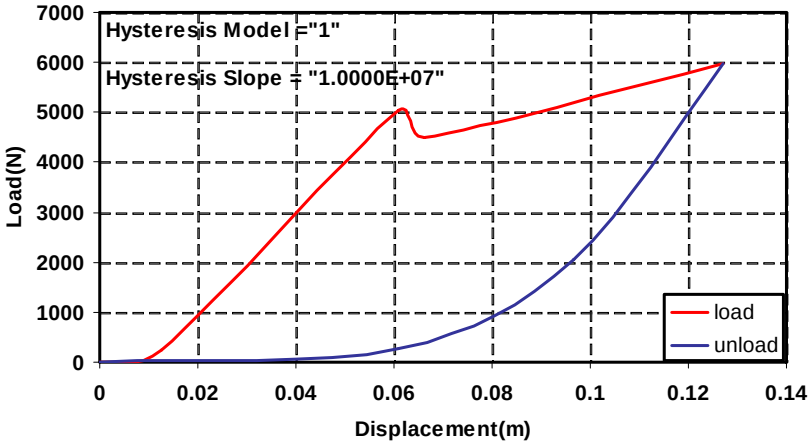

Figure 18. Load Displacement for Panel Used for Test 01057-82

The resulting head acceleration profiles for the NHCT test and the corresponding MADYMO model are shown in figure 19. As can be seen, they indicate a reasonable level of correlation. Table 6 summarizes the outputs of both data sets.

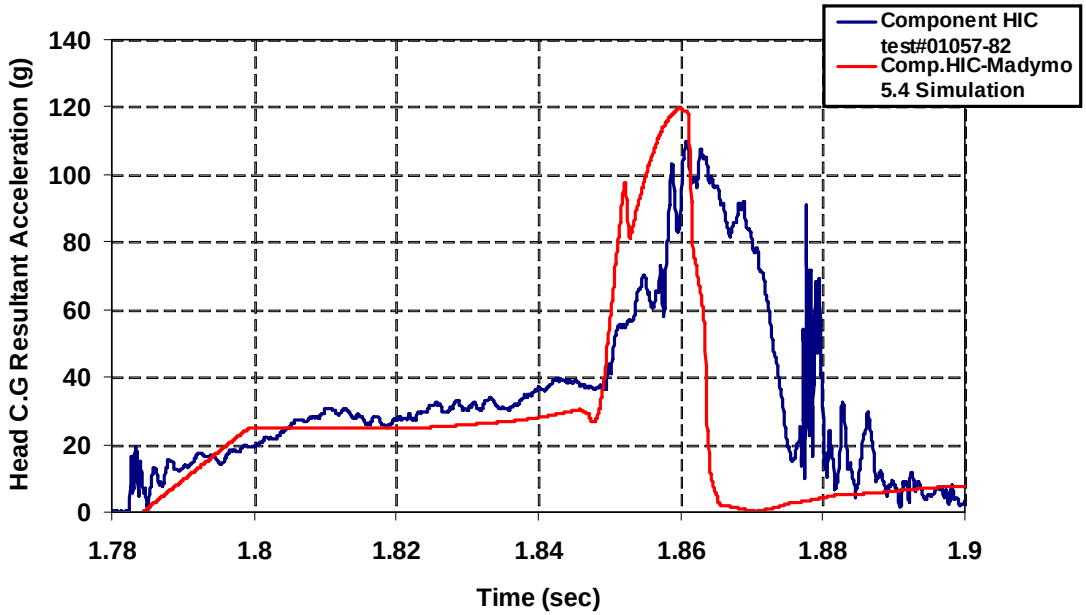

Figure 19. Head Acceleration Profiles for MADYMO Model and NHCT Test 01057-82

Table 6. Comparison of NHCT Test 01057-82 With MADYMO Simulation

Parameters	NHCT Test 01057-82	MADYMO Simulation
Head impact angle (deg)	40.0	40.0
Head impact velocity (ft/sec)	46.0	46.1
HIC	1271.0	1222.0
HIC window (ms)	22.6	22.6
Head c.g. peak acceleration (g's)	110.0	117.0
Head c.g. avg. acceleration (g's)	79.3	90.1

Other NHCT tests were also compared with the MADYMO model. The model again indicated a reasonable level of correlation. A similar set of comparative tests is described in section 8.2.2.

6.2 MADYMO MODEL SETUP FOR THE FSST.

A MADYMO model was developed for several FSSTs. As a representation, the model developed for FSST 97191-003 is shown in figure 20. The seat setback distance was 34 inches and the identical Nomex honeycomb panel, with vertical slits 4 inches apart, was used in the FSST. The same properties were used in the MADYMO models as used in the NHCT test. The head impact angle and velocity obtained from the sled test were 40 degrees and 46 ft/sec respectively. The seat was developed using planes in the reference space along with the panel. A Hybrid II ATD was positioned on the seat with the desired orientation. The friction used between the ATD, seat, and panel was 0.3. The loading and unloading curves for the panels are shown in figure 21.

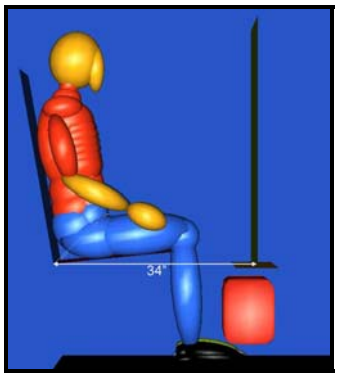

Figure 20. MADYMO Model Setup for FSST 97191-003

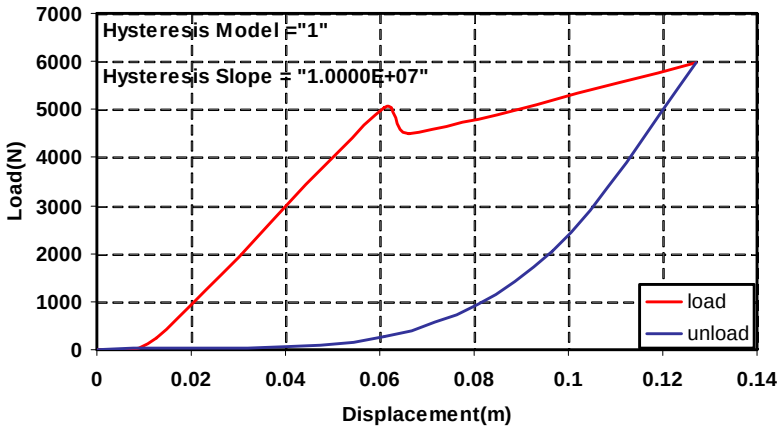

Figure 21. Load Displacement for Slitted Panel

The MADYMO model required the use of a lap belt. The properties of the MADYMO belt used for this purpose are shown in figure 22. The hysteresis is produced following portions of the loading and unloading curve as defined in MADYMO [12]. The input pulse for the MADYMO model is shown in figure 23.

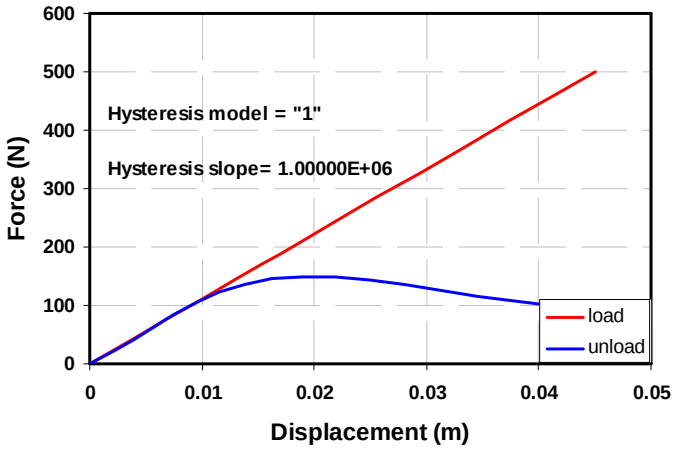

Figure 22. Load Displacement for MADYMO Belt Used

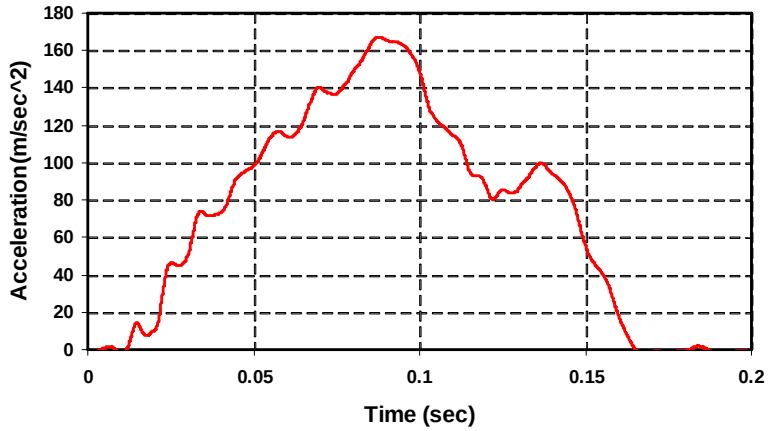

Figure 23. Input Pulse for FSST MADYMO Model

The head acceleration profiles for both the FSST as well as the MADYMO model were compared in figure 24 and observed to match quite closely. The outputs from both sets of data are listed in table 7 and indicate that the MADYMO model can be used to evaluate the FSST with a reasonable level of confidence. This MADYMO model has also been used in another set of comparative tests in section 8.2.1.

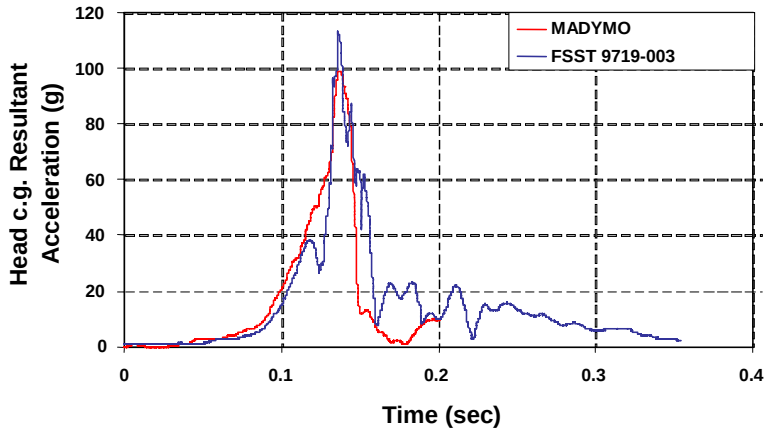

Figure 24. Head Acceleration Profile for MADYMO Model and FSST 9719-003

Table 7. Comparison of FSST 97191-003 With MADYMO Simulation

Parameters	FSST 97191-003	MADYMO Simulation
Head impact angle (deg)	40.0	40.0
Head impact velocity (ft/sec)	46.0	46.1
HIC	1131.0	1220.0
HIC window (ms)	22.6	22.6
Head c.g. peak acceleration (g's)	113.2	99.3
Head c.g. avg. acceleration (g's)	76.1	67.6

6.3 PARAMETRIC STUDY OF IMPACT SURFACE STIFFNESS AND SETBACK DISTANCES.

Using the two previous FSST and NHCT MADYMO models, a parametric study of both systems was conducted with the intent of understanding the dynamic response of NHCT for different scenarios, and to develop a correlation model between the FSST and NHCT. The results show that for a given setback distance, HIC increases with an increase in stiffness of the impact surface panel.

6.3.1 Parametric Study With FSST.

This section describes a parametric study conducted using the MADYMO model derived from sled tests using ETHAFOAM™ panels. This study was conducted with the intent of understanding the effect of panel stiffness and impact angle on the dynamic behavior of NHCT. The setup of the MADYMO model is shown in figure 25. A model with a range of assumed linear values was used to represent stiffness properties (linear force deflection properties) of the impact surface. Figure 26 shows the load-deflection properties of the panel.

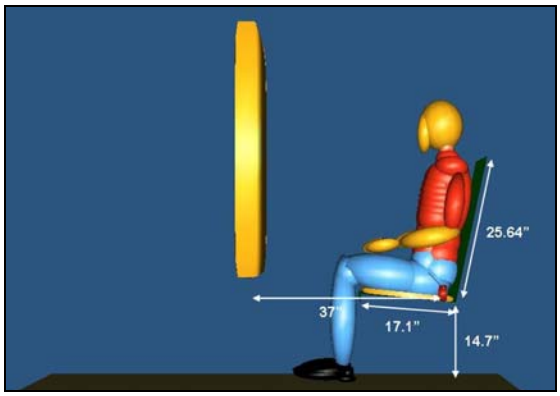

Figure 25. Setup of the MADYMO With ETHAFOAM Panel

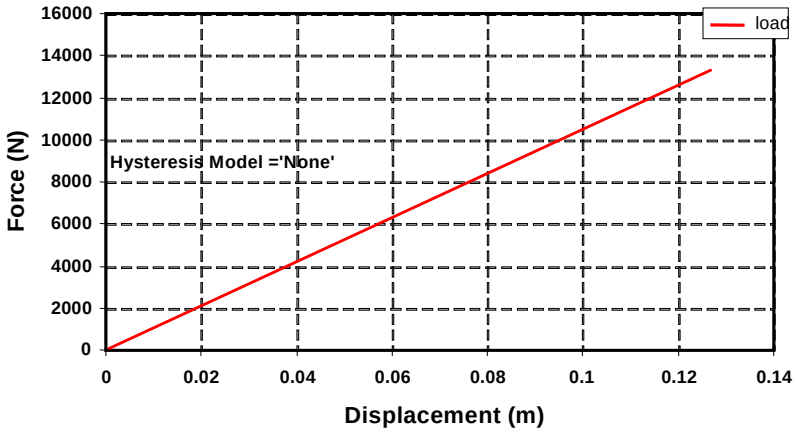

Figure 26. Linear Load Deflection Properties of the ETHAFOAM Panel

The input pulse for all the simulations used the standard triangular Federal Aviation Administration (FAA) 16-g, 180-ms pulse as shown in figure 27. Figure 28 shows the MADYMO lap belt properties, while figure 29 shows the properties of the seat cushion.

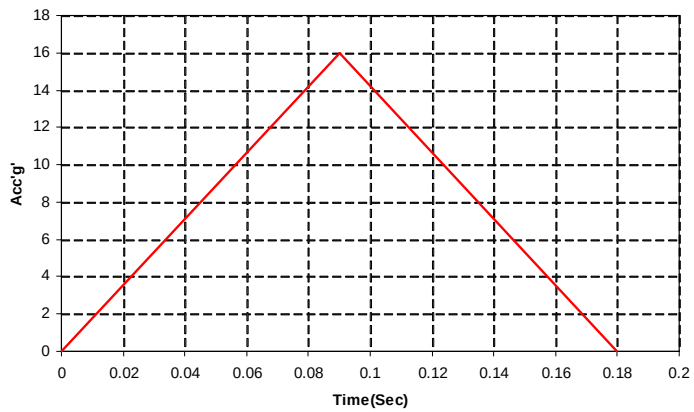

Figure 27. MADYMO Simulation Input Pulse

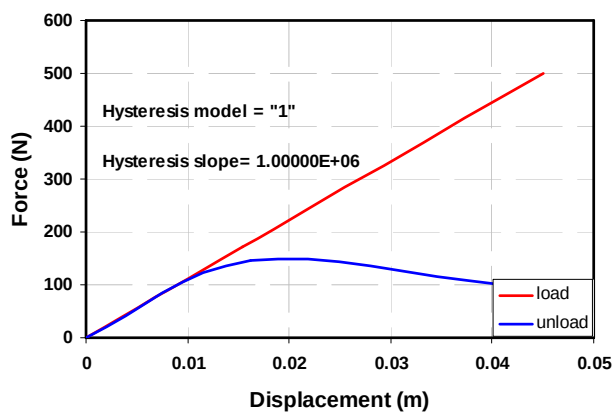

Figure 28. MADYMO Lap Belt Load Deflection Properties

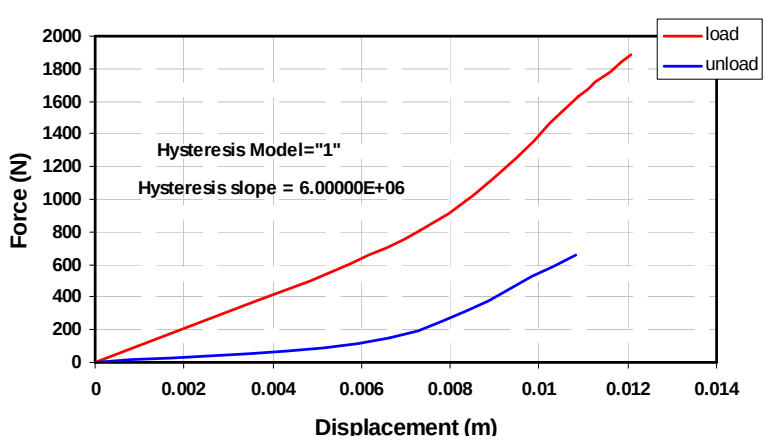

Figure 29. Seat Cushion Load Deflection Properties

Figure 30 shows the MADYMO model simulation sequence. The results of the parametric study are shown in table 8.

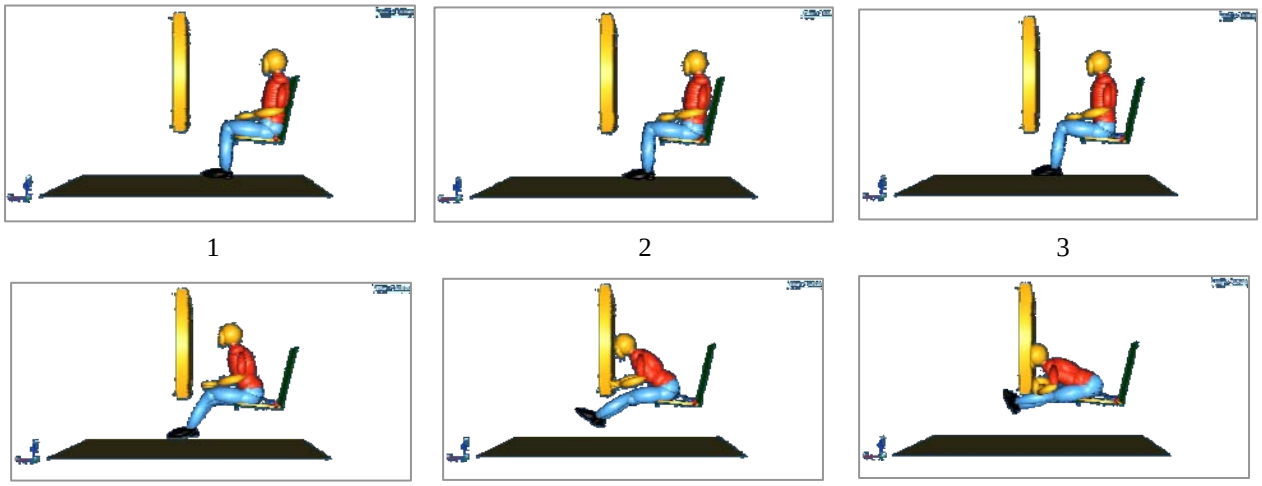

1 2 3

4 5 6

Figure 30. Simulation of the FSST With ETHAFOAM Panel

Table 8. The FSST Simulation Results of Panel Stiffness and Impact Angles

Impact Angle		Stiffness (lb/in.)							
		50	100	150	200	300	400	500	600
31 (deg)	HIC	210 [Δt=15ms]	435 [Δt=15ms]	721 [Δt=9ms]	968 [Δt=10ms]	1619 [Δt=11ms]	2111 [Δt=9ms]	2616 [Δt=8ms]	3114 [Δt=15ms]
	HIC window								
40 (deg)	HIC	160 [Δt=15ms]	340 [Δt=15ms]	670 [Δt=11ms]	1044 [Δt=13ms]	1491 [Δt=11ms]	1931 [Δt=11ms]	2377 [Δt=9ms]	2771 [Δt=8ms]
	HIC window								
53 (deg)	HIC	120 [Δt=15ms]	228 [Δt=15ms]	387 [Δt=15ms]	503 [Δt=15ms]	721 [Δt=13ms]	916 [Δt=13ms]	1112 [Δt=11ms]	1293 [Δt=9ms]
	HIC window								

6.3.2 Parametric Study With NHCT.

As was the case for the FSST, a parametric study was carried out for the NHCT MADYMO model. The NHCT model was validated using NHCT test 01057-82. The panel was given the same load deflection curve as that used in the simulation of previous sled tests. The simulation sequence is shown in figure 31. A series of simulations was conducted with similar panel properties and head impact angles as used for the previous sled test to study the effect of these factors on the HIC value. Moving the panel closer to or away from the tester changed the impact angle. The data from these tests are listed in table 9.

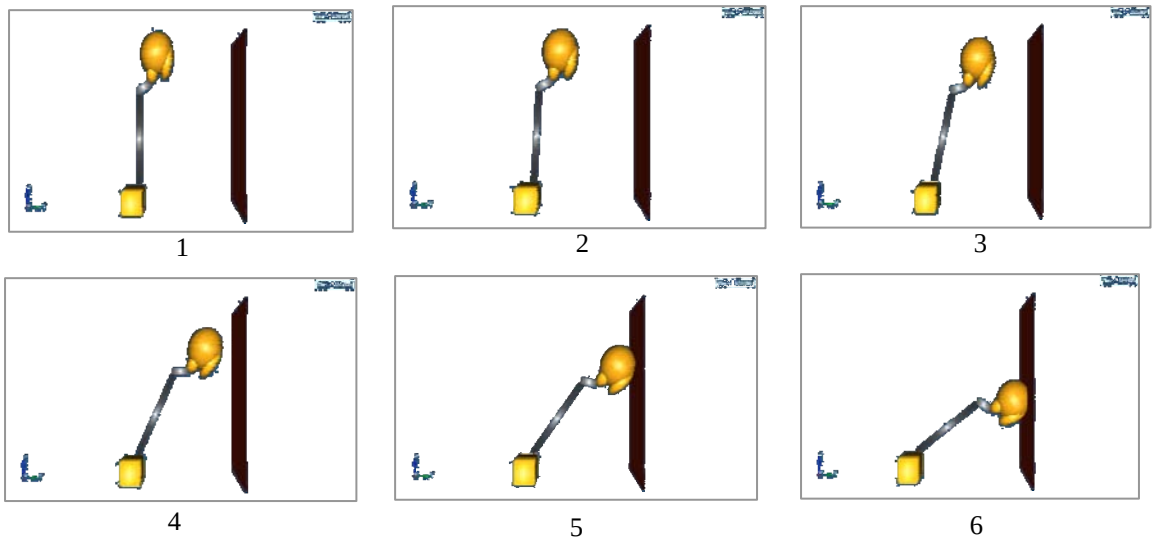

Figure 31. Simulation Sequence for Impact Angle of 53 Degrees With ETHAFOAM Panel for the NHCT

Table 9. Simulation Results of Panel Stiffness and Impact Angle for the NHCT

Impact Angle		Stiffness (lb/in)							
		50	100	150	200	300	400	500	600
31 (deg)	HIC	283	714	1040	1280	1771	2181	2774	3154
	HIC window	[Δt=15ms]	[Δt=15ms]	[Δt=13ms]	[Δt=11ms]	[Δt=15ms]	[Δt=8ms]	[Δt=6ms]	[Δt=6ms]
40 (deg)	HIC	159	525	850	1152	1589	2020	2390	2733
	HIC window	[Δt=15ms]	[Δt=15ms]	[Δt=15ms]	[Δt=13ms]	[Δt=10ms]	[Δt=15ms]	[Δt=7.0ms]	[Δt=7.0ms]
53 (deg)	HIC	48	164	347	536	884	1191	1488	1776
	HIC window	[Δt=15ms]	[Δt=15ms]	[Δt=15ms]	[Δt=15ms]	[Δt=15ms]	[Δt=13ms]	[Δt=11ms]	[Δt=10ms]

From the results of the parametric studies listed in tables 8 and 9, the HIC is inversely proportional to the impact angle. This correlation is depicted in the following section.

6.4 CORRELATION OF MADYMO MODELS FOR FSST AND NHCT.

Correlation for impact angles of 31, 40, and 53 degrees was performed for the NHCT and FSST MADYMO models.

6.4.1 Panel Stiffness and HIC at an Impact Angle of 31 Degrees.

Figure 32 shows the relationship between the panel stiffness and HIC value for the NHCT and the FSST at an impact angle of 31 degrees. The HIC values for the NHCT and the FSST were calculated using the coefficients derived in MADYMO (equations 1 and 2).

$$HIC_{NHCT} = 5.54\,K \quad (1)$$
$$HIC_{FSST} = 5.22\,K \quad (2)$$

where: K = Stiffness of the panel (lb/in.)

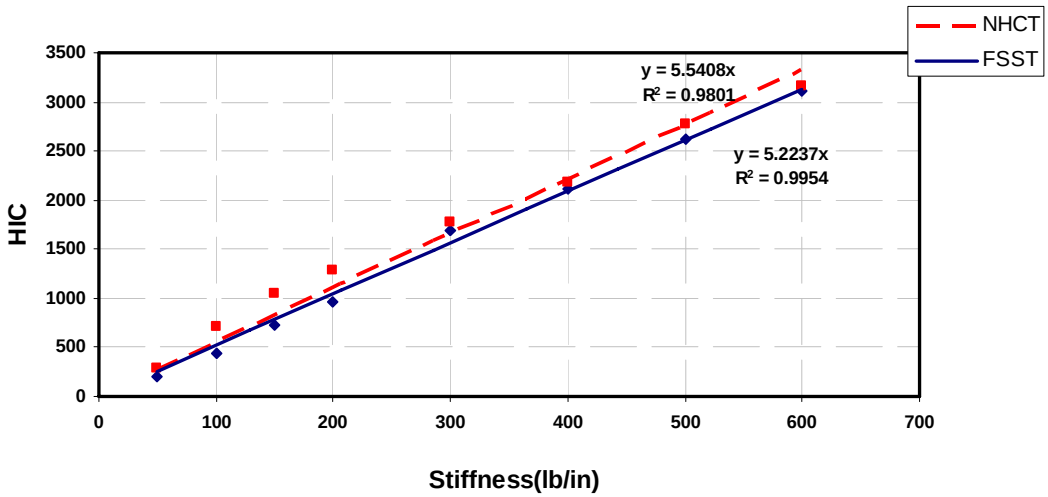

Figure 32. The HIC Correlation for FSST and NHCT MADYMO ModelsWith an Impact Angle of 31 Degrees

The equations obtained can be used to predict the HIC relationship between the NHCT and the FSST (equation 3).

$$\frac{HIC_{NHCT}}{HIC_{FSST}} = 1.06 \tag{3}$$

This relationship applies when the head impact angle is 31 degrees and corresponding pivotal setback distance for the NHCT is 18 in. (seat setback distance of 28 in.).

6.4.2 Panel Stiffness and HIC at an Impact Angle of 40 Degrees.

Figure 33 shows the relationship between the panel stiffness and HIC value for the NHCT and the FSST at an impact angle of 40 degrees. The HIC values for the NHCT and the FSST were calculated using the coefficients derived in MADYMO (equations 4 and 5).

$$HIC_{NHCT} = 4.84\ K \tag{4}$$
$$HIC_{FSST} = 4.72\ K \tag{5}$$

where: K = Stiffness of the panel (lb/in.)

The equations obtained can be used to predict the HIC relationship between the NHCT and the FSST (equation 6).

$$\frac{HIC_{NHCT}}{HIC_{FSST}} = 1.02 \tag{6}$$

This relationship applies when the head impact angle is 40 degrees and corresponding pivotal setback distance for the NHCT is 22.5 in. (seat setback distance of 32 in.).

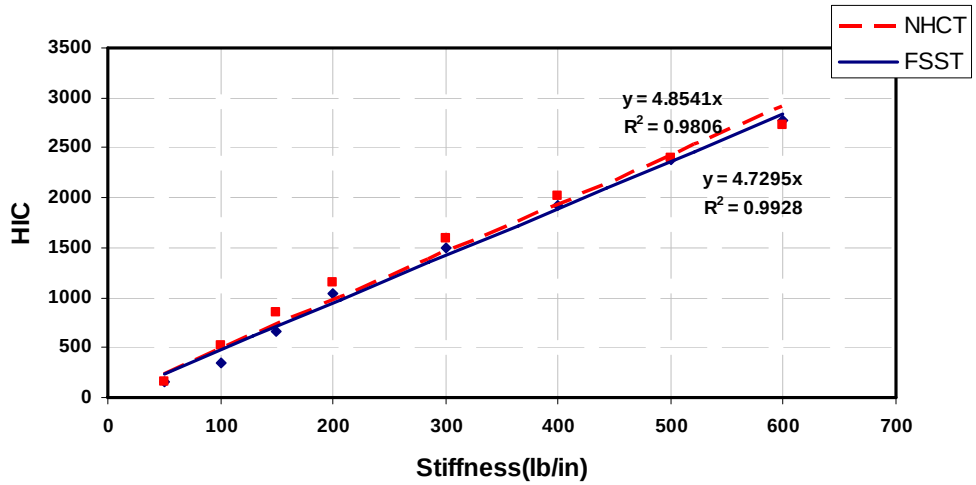

Figure 33. The HIC Correlation for FSST and NHCT MADYMO Models With an Impact Angle of 40 Degrees

6.4.3 Panel Stiffness and HIC at an Impact Angle of 53 Degrees.

Figure 34 shows the relationship between the panel stiffness and HIC value for the NHCT and the FSST at an impact angle of 53 degrees. The HIC values for the NHCT and the FSST were calculated using the coefficients derived in MADYMO (equations 7 and 8).

$$HIC_{NHCT} = 2.91\ K \tag{7}$$
$$HIC_{FSST} = 2.24\ K \tag{8}$$

where: K = Stiffness of the panel (lb/in.)

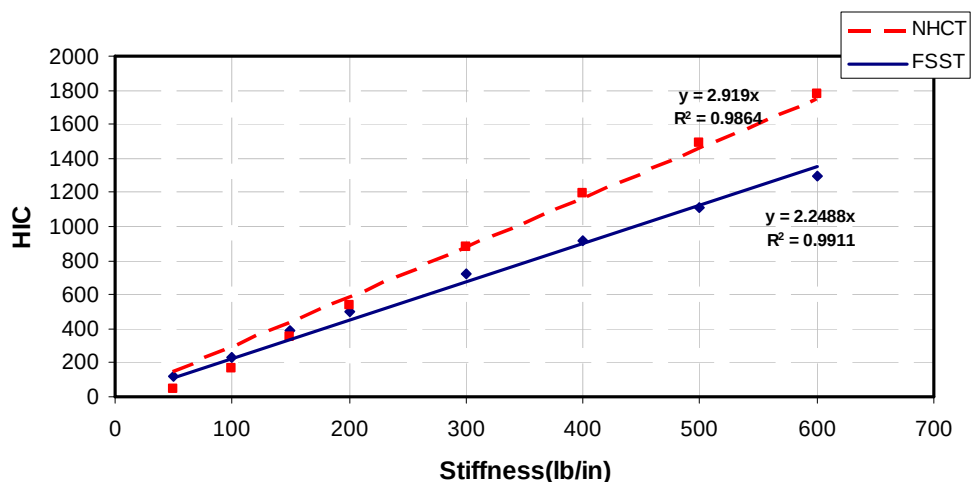

Figure 34. The HIC Correlation for FSST and NHCT MADYMO Models With an Impact Angle of 53 Degrees

The equations obtained can be used to predict the HIC relationship between the NHCT and the FSST (equation 9).

$$\frac{HIC_{NHCT}}{HIC_{FSST}} = 1.29 \tag{9}$$

This relationship can be used when the head impact angle is 53 degrees and the corresponding pivotal setback distance for the tester is 27.5 in. (seat setback distance of 37 in.).

6.4.4 Correlation of FSST and NHCT HIC Models.

Figure 35 shows a plot of the correlation between the FSST and NHCT models for various impact angles. The plot shows a reasonable correlation at higher impact angles but with a trend towards the NHCT overpredicting at lower impact angles.

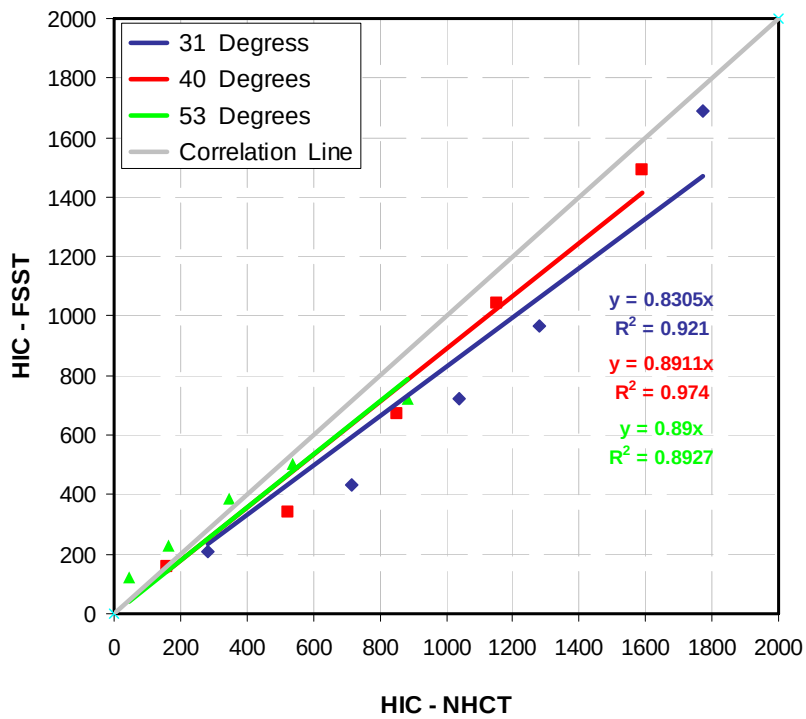

Figure 35. Comparison of MADYMO Models of HIC-FSST vs HIC-NHCT for 31-, 40-, and 53-Degree Impact Angles (Seat setback of 28, 32, and 37 inches)

Results from the parametric study indicate that the NHCT overpredicts the FSST, and thus provides conservative values. The amount of overprediction depends on the seat setback distance or the head impact angle. Generally, the device produces most conservative results compared to the FSST for small seat setback distances or small head impact angle.

7. SUMMARY OF CAMI NHCT TESTS.

A series of sled tests and NHCT tests were conducted at Civil Aerospace Medical Institute (CAMI) with the intent of evaluating the performance of the NHCT with various aircraft interior surfaces, as depicted in figure 36. All tests were conducted at various impact velocities and impact angles that could be encountered during certification tests. MADYMO modeling and analysis were used to determine the critical input parameters, such as impact angle, impact velocity, and point of impact on the surface, which greatly reduced the number of trial runs. The sled test was carried out using a Hybrid II ATD positioned on a rigid seat with a lap belt. Photometric analysis was used to acquire the impact velocity, impact angle, and point of impact for the sled tests. Table 10 [12] summarizes the results of various sled tests and corresponding NHCT tests for different impacting surfaces. Some surfaces used for the tests included a polyethylene foam pad (ETHAFOAM), fiberglass-faced aluminum honeycomb, and fiberglass-faced Nomex honeycomb along with energy absorbing seat backs with and without video displays.

Figure 36. Different Impact Surfaces Used for CAMI Tests

Table 10. Results of the FSST and NHCT Test Using Different Impact Surfaces

Surface	Test ID	Head Velocity (ft/sec)	Impact Angle (degree)	HIC	HIC Duration (ms)
Polyethylene foam pad (ETHAFOAM)	A03007	32.2	45.7	304	28
	A03008	32.6	46.7	302	29
	H03316	28.3	43.0	400	19
	A03011	38.7	40.6	667	17
	A03013	38.7	40.6	699	21
	H03314	36.9	43.0	756	18
	A03009	42.4	41.6	1047	16
	A03010	43.8	42.9	1044	16
	H03315	40.3	43.0	918	23
	H03317	39.5	43.0	942	15
	H03318	39.0	43.0	873	17
	H03319	39.3	43.0	923	17
Fiberglass-faced, aluminum honeycomb	A03022	42.1	42.4	772	20
	H03322	41.9	42.4	726	26
	A03023	46.3	38.4	1009	21
	H03329	45.8	37.9	802	26
Narrow, fiberglass-faced Nomex honeycomb panel	A03015	38.0	44.6	1110	17
	A03018	37.9	44.1	944	16
	H03325	37.7	44.9	389	5
Wide, fiberglass-faced, Nomex honeycomb panel	A03004	44.7	53.2	1084	7
	H03320	47.6	53.0	1420	23
Narrow-body class divider panel	A03028	41.6	43.8	458	34
	H03330	41.6	44.0	285	36
Wide-body class divider panel	A03027	40.5	45.8	1547	5
	A03034	41.3	49.5	1597	11
	H03331	40.8	44.0	670	9
SEAT BACK TESTS					
Seatback centered	A04075	47.4	38.5	1207	29
	A04076	48.0	38.7	1179	25
	A04077	47.4	38.9	1225	10
	H04304	51.5	40.0	819	12
	H04305	51.6	40.0	804	12
	H04306	50.5	40.0	818	12
Seatback offset	A04081	49.2	41.4	867	7
	A04082	48.1	42.9	907	7
	A04083	48.8	42.8	801	11
	H04307	51.0	42.6	737	17
	H04308	50.0	42.6	881	19
	H04309	49.2	42.6	674	7

Note: FSST ID numbers start with A. NHCT ID numbers start with H.

8. EVALUATION OF NHCT TESTS CONDUCTED AT CAMI.

It is generally known that HIC is quite sensitive to input parameters such as head impact angle, head impact velocity, and impact location. MADYMO models have shown that minor changes in the input parameters, such as impact angle and velocity, can result in noticeable variations in the resulting HIC values.

The FSST and NHCT tests conducted at CAMI (table 10) were originally intended to be used on a one-to-one basis to evaluate the correlation of the resulting HIC values from the two systems. However, some level of difficulty was encountered in matching the input parameters for both systems, i.e., the tests were not carried out under identical conditions. This resulted in most of the FSST parameters having some degree of variation from their corresponding NHCT tests that would possibly contribute a sizable degree of uncertainty to any one-to-one comparison carried out as originally envisaged.

In view of this, it became necessary to devise a methodology that would make it possible to obtain sets of data that could be compared on a one-to-one basis. This was done using a analytical-experimental modeling process, as outlined in figure 37 and detailed below. This study also gave an indication of the substantial variations in HIC caused by minor variations in test conditions.

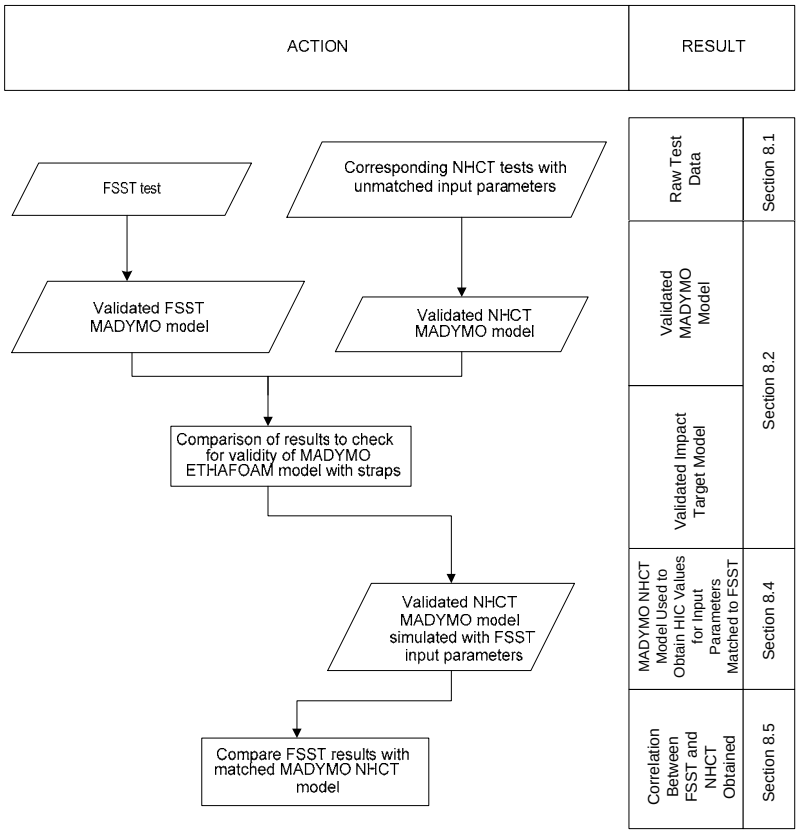

Figure 37. Process Flow for Analytical-Experimental Model

8.1 RAW TEST DATA.

The raw data used for this process was obtained from the test results from table 10. The impact surface used was ETHAFOAM, which represented the heavily padded interior surface of an aircraft structure. The ETHAFOAM used was 4 inches thick and possessed a smooth surface, as shown in figure 38. The corresponding NHCT test, which was conducted to match the FSST, is shown in figure 39.

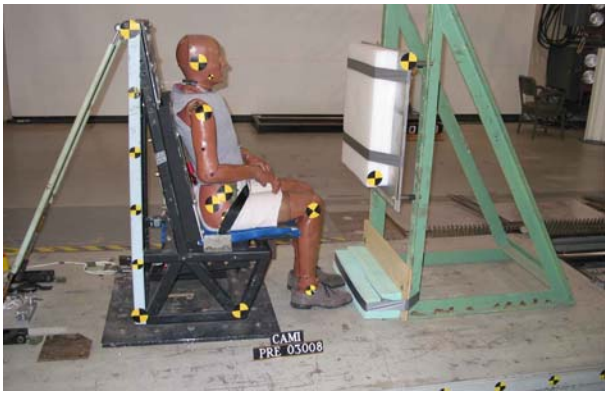

Figure 38. ETHAFOAM Setup for FSST A03007

Figure 39. Corresponding NHCT Test for FSST A03007

The corresponding input parameters are shown in table 11. As noted, some variation in the input parameters occurs.

Table 11. FSST and NHCT Tests With ETHAFOAM Impact Surface

Test ID	Head Velocity (ft/sec)	Impact Angle (degree)	HIC	HIC Duration (ms)
A03007	32.2	45.7	304	28
H03316	28.3	43.0	400	19

Note: FSST ID numbers start with A. NHCT ID numbers start with H.

8.2 VALIDATED MADYMO NHCT AND FSST MODELS.

Separate MADYMO models were developed for both the NHCT and FSST using identical ETHAFOAM targets secured to a rigid surface using duct tape as detailed in the next section.

8.2.1 Validation of FSST MADYMO Model.

The tests were simulated using a MADYMO 50th percentile Hybrid II ATD. The finite element (FE) model of polyethylene foam pad was modeled using solid elements. The duct tape holding the foam with the rigid support was modeled as straps (Kelvin elements) with a stiffness of 2×10^6 N/m, to hold the FE foam on the rigid FE surface, as shown in figure 40. A MADYMO seat belt was used to restrain the ATD. The seat back and pan were simulated using planes, while the cushion itself was represented by a 1-inch-thick ellipsoid with the same properties as used at CAMI. The setup is shown in figure 41. The simulation was carried out to validate the MADYMO model for test A03007.

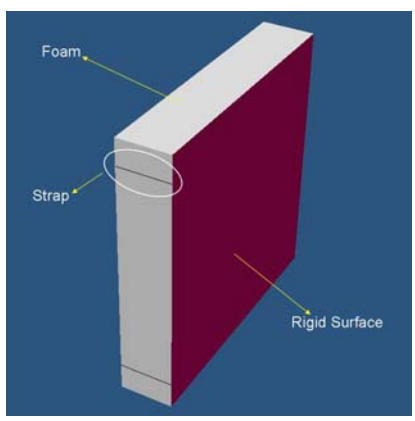

Figure 40. Finite Element Model of Polyethylene Foam Pad With Duct Tape (Straps)

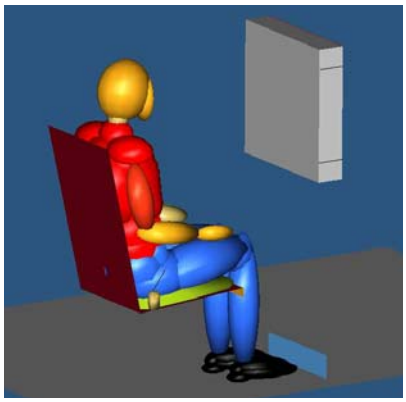

Figure 41. MADYMO Model Developed for FSST

The input acceleration pulse was obtained from the accelerometer output from the actual CAMI FSST A03007. This is shown in figure 42.

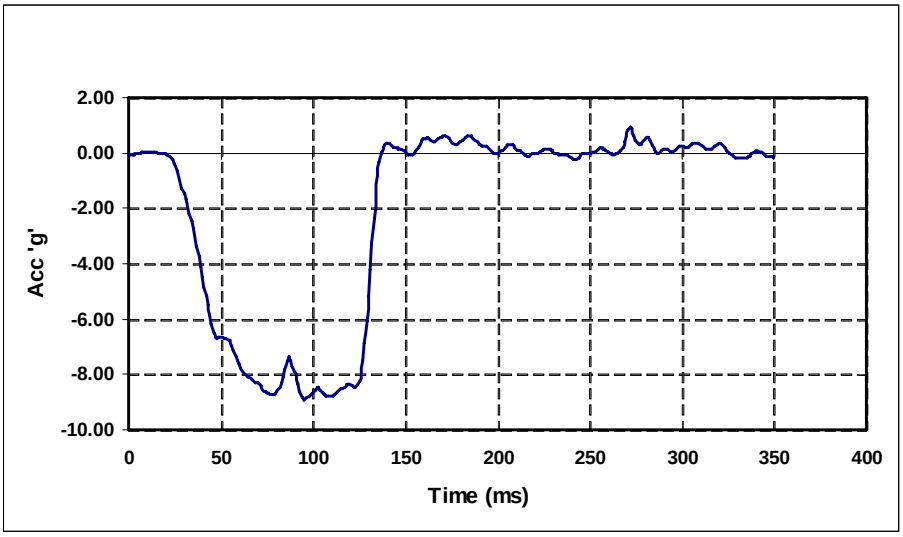

Figure 42. Acceleration Pulse for FSST A03007

The belt properties used for the FSST A03007 are the same ones that were used for the FSST model in section 6.2. The load deflection properties of the foam are shown in figure 43. The MADYMO model used hysteresis model 2 setting.

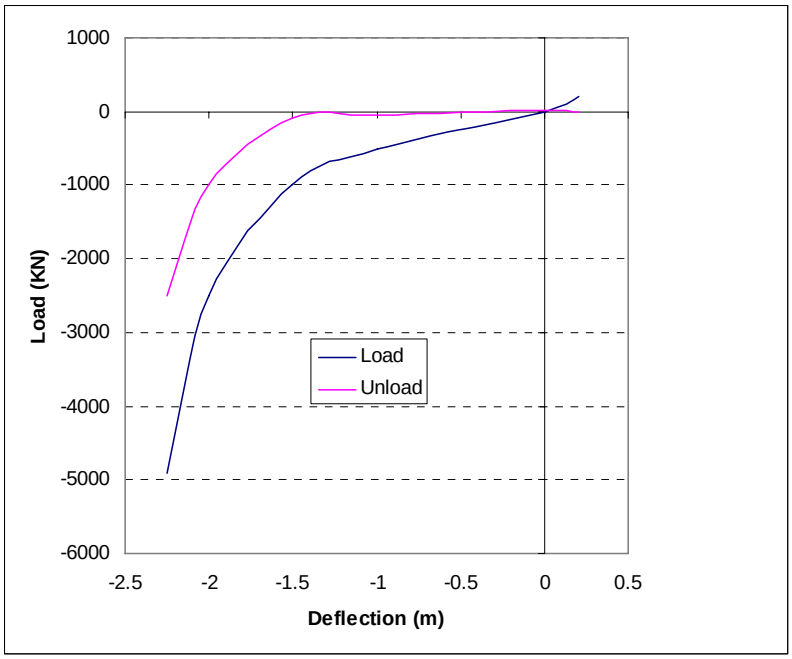

Figure 43. Foam Load Deflection Properties

A sequence of the resulting simulation of the MADYMO model is shown in figure 44.

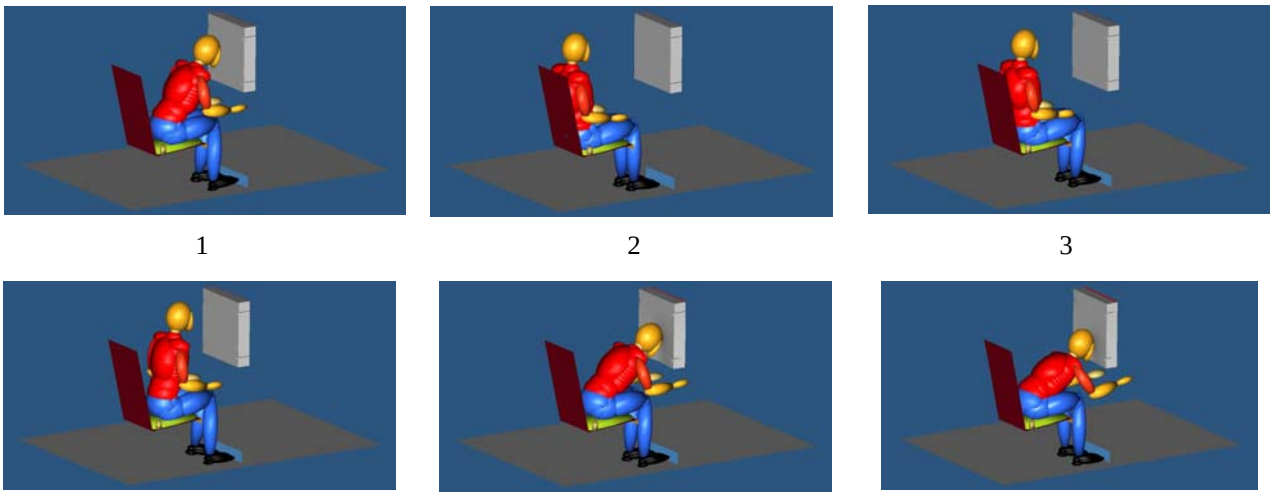

Figure 44. Simulation Sequence for Head Strike for FSST A03007

The ensuing deformation and slip of the MADYMO model of the ETHAFOAM target is shown in figure 45. This response is very close to that observed during actual head impact in FSST.

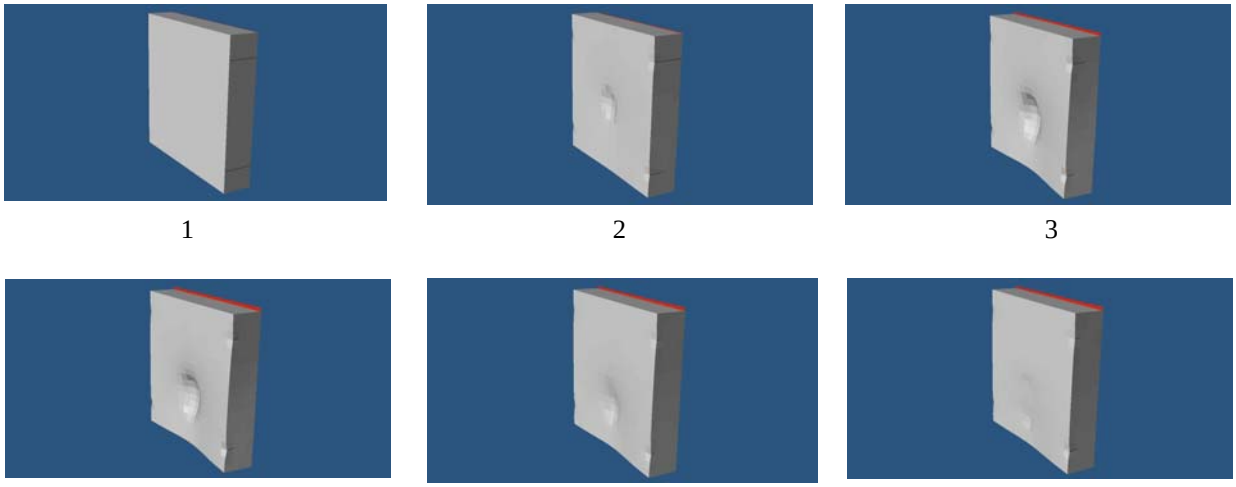

Figure 45. Simulation Sequence of Foam Deformation and its Relative Motion With Rigid Surface for FSST A03007

Figure 46 shows a comparison of the resulting head acceleration profile of the FSST and the MADYMO model. As can be seen, they show a reasonable degree of correlation.

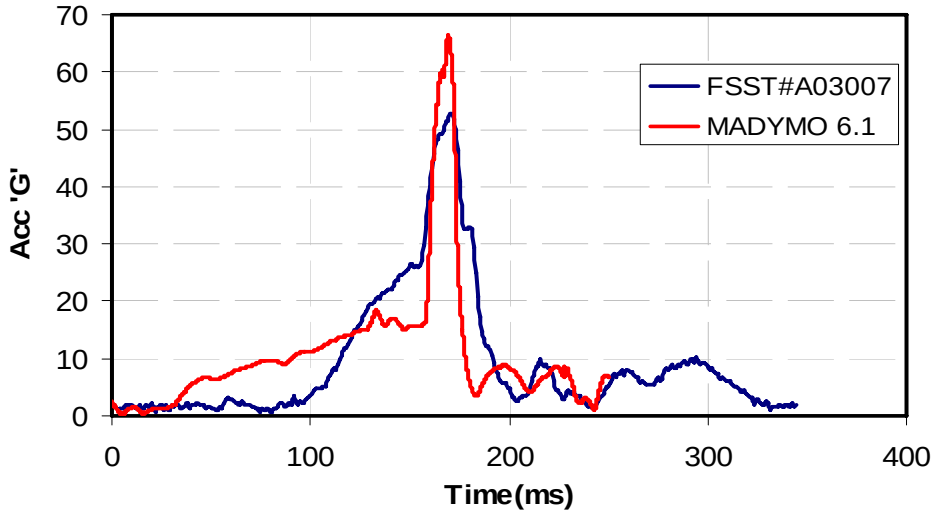

Figure 46. Head Acceleration for FSST and MADYMO Model

The FSST and MADYMO results are summarized in table 12. The outputs appear to be almost identical, indicating a very significant level of correlation that is indicative of an MADYMO model with a high-fidelity level. A similar validation for the FSST model was carried out in section 6.2 for test 97191-003.

Table 12. Comparison of FSST A03007 With MADYMO Simulation

Parameters	FSST A03007	MADYMO Simulation
Head impact angle (deg)	45.7	45.5
Head impact velocity (ft/sec)	32.2	32.1
HIC	304.0	315.0
HIC window (ms)	28.0	28.0
Head c.g. peak acceleration (g's)	52.0	65.0
Head c.g. avg. acceleration (g's)	33.0	28.0

8.2.2 Validation of NHCT MADYMO Model.

The NHCT MADYMO model used the same input parameters and impact target as NHCT test H03316. The resulting simulation sequence and target dynamics are shown in figures 47 and 48.

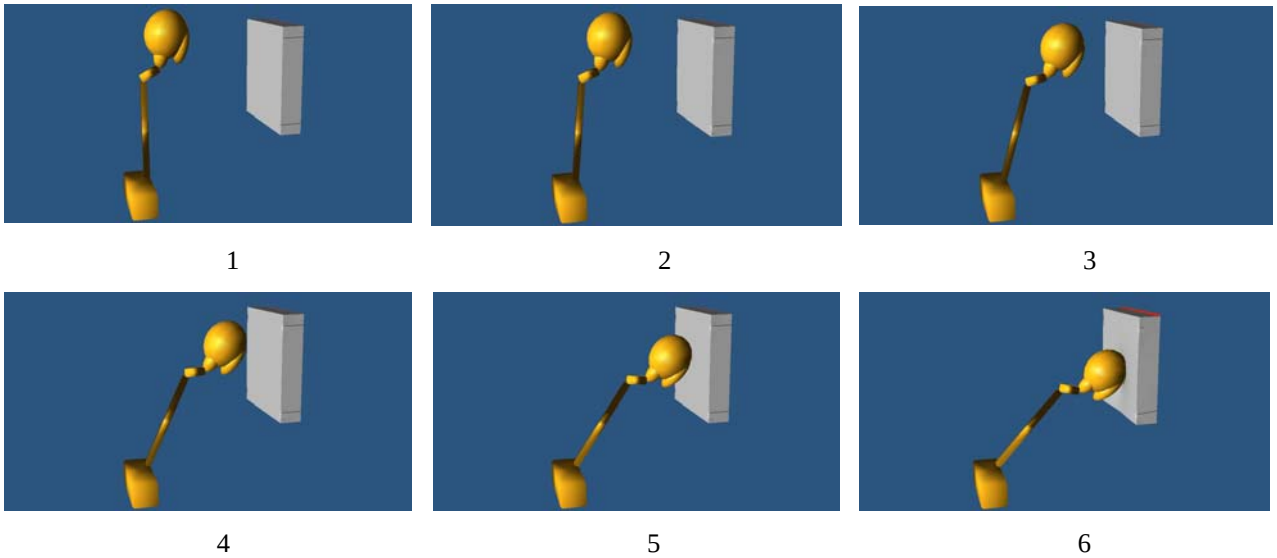

Figure 47. Simulation Sequence for Head Strike NHCT Test H03316

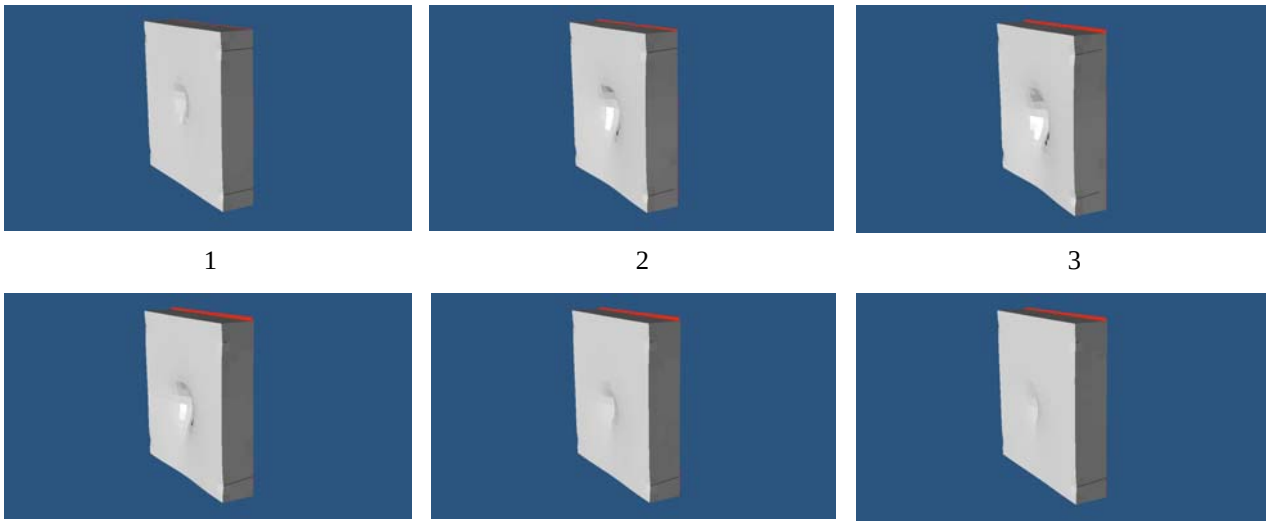

1 2 3

4 5 6

Figure 48. Simulation Sequence of Foam Deformation and its Relative Motion With Rigid Surface for NHCT Test H03316

Figure 49 shows a comparison of the resulting head acceleration profile of the NHCT and the corresponding MADYMO model, which are similar. The resulting output parameters are tabulated in table 13. A very significant correlation of the outputs and hence conformation of a high-fidelity model can be noted. A similar validation sequence for this model was carried out in section 6.1 for NHCT test 01057-82.

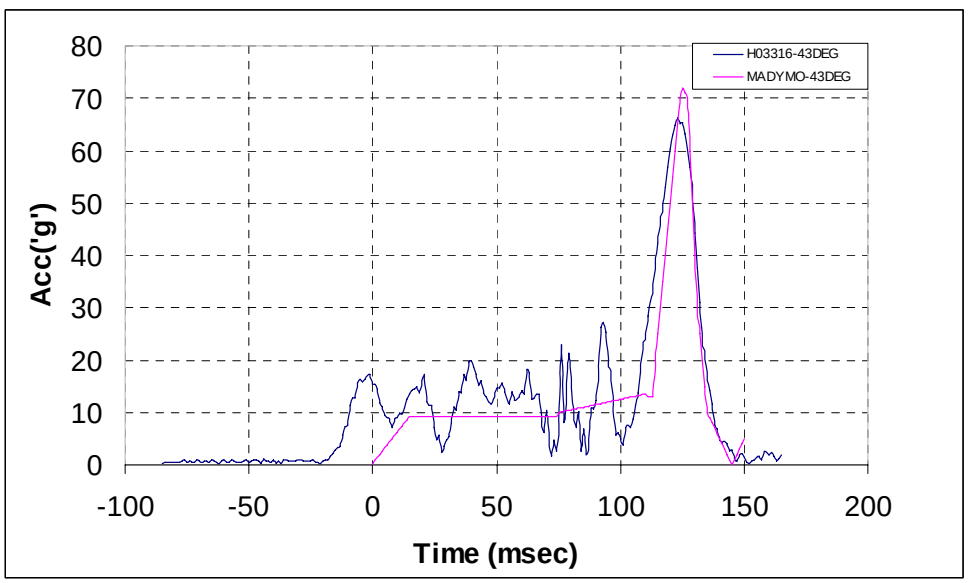

Figure 49. Head Acceleration Profile for Actual Test and Simulation

Table 13. Comparison of NHCT Test H03316 With MADYMO Simulation

Parameters	NHCT Test H03316 43 degree	MADYMO Simulation
Head impact angle (deg)	43.0	43.0
Head impact velocity (ft/sec)	28.3	28.3
HIC	400.0	408.0
HIC window (ms)	19.0	15.0
Head c.g. peak acceleration (g's)	66.0	71.0
Head c.g. avg. acceleration (g's)	30.2	29.0

8.3 USE OF MADYMO NHCT MODEL TO OBTAIN HIC VALUES FOR INPUT PARAMETERS MATCHED TO FSSTS.

As noted earlier, the input parameters of the FSST and their corresponding NHCT tests would appear to differ to a level sufficient to cast some level of uncertainty on the results of any correlation carried out between these two sets of data. This data is tabulated in table 14.

Table 14. Comparison of HIC Results for FSST and NHCT

FSST				NHCT Test			
Test ID	Head Velocity (ft/sec)	Impact Angle (degree)	HIC	Test ID	Head Velocity (ft/sec)	Impact Angle (degree)	HIC
A03007	32.2	45.7	304.3				
				H03316	28.3	43	400.8
A03008	32.6	46.7	302.1				
A03009	42.4	41.6	1047.2	H03317	39.5	43	946.6
A03010	43.8	42.9	1044.5	H03315	40.3	43	918.9
A03011	38.7	40.6	667.9	H03314	36.9	43	756.3

Note: FSST ID numbers start with A. NHCT ID numbers start with H.

The validated MADYMO model of the NHCT and ETHAFOAM panel developed in the previous section were used to carry out a set of simulations to obtain output values for the NHCT for input values exactly corresponding to those of the FSSTs. The results of this process are tabulated in table 15. The HIC calculation was made using unlimited HIC.

Table 15. Comparison of HIC Results for FSST and MADYMO NHCT

FSST Test				MADYMO Model of NHCT			
Test ID	Head Velocity (ft/sec)	Impact Angle (degree)	HIC	Test ID	Head Velocity (ft/sec)	Impact Angle (degree)	HIC
A03007	32.2	45.7	304.3	H03007	32.2	45.7	439.6
A03008	32.6	46.7	302.1	H03008	32.6	46.7	405.4
A03009	42.4	41.6	1047.2	H03009	42.4	41.6	1390.4
A03010	43.8	42.9	1044.5	H03010	43.8	42.9	1234.7
A03011	38.7	40.6	667.9	H03011	38.7	40.6	1203

Note: FSST ID numbers start with A. Corresponding MADYMO NHCT ID numbers start with H.

8.4 CORRELATION BETWEEN FSST RESULTS AND MADYMO NHCT RESULTS.

A plot of FSST and MADYMO NHCT model results is shown in figure 50. The MADYMO NHCT model consistently produces conservative results compared to the FSST. The MADYMO NHCT model and NHCT overpredicts the HIC compared to the FSST.

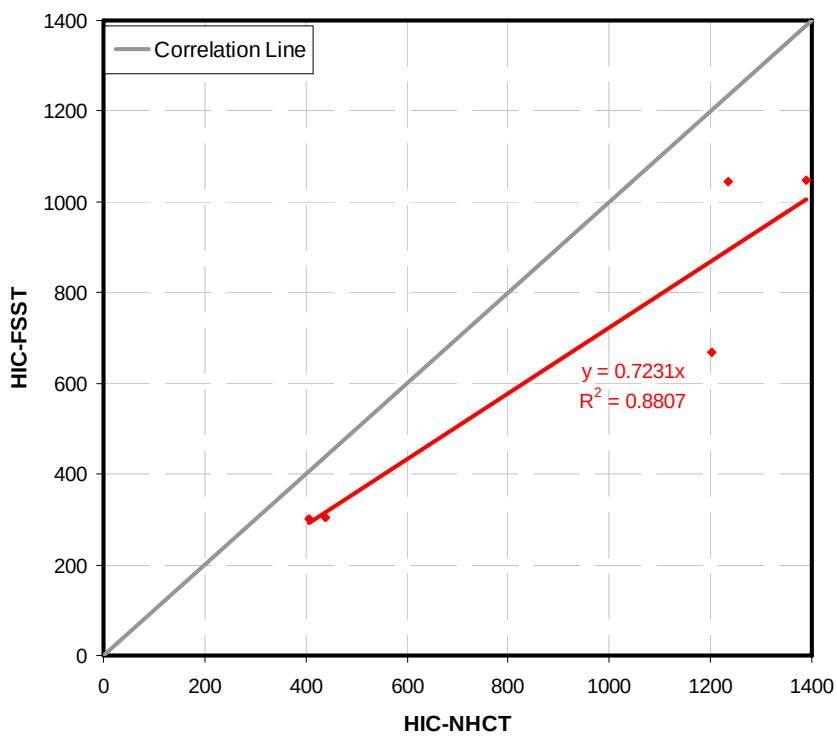

Figure 50. Correlation of MADYMO NHCT and FSST

9. EVALUATION OF NHCT WITH A FLEXIBLE NECK.

A substantial amount of head rotation for the Hybrid II ATD was observed after impacting the various surfaces with different head impact angles. The NHCT in its current configuration is incapable of replicating this effect. A study using a mathematical model was carried out with the intent of understanding the modification required, addressing this issue and its efficacy in improving the dynamic response of NHCT. The same NHCT model as used in the previous sections was used with the exception of the rigid neck being swapped out for a flexible one.

The tests were simulated using a MADYMO 50th percentile male Hybrid II ATD. An ETHAFOAM panel with stiffness of 600 lb/in. was modeled using a 4-inch ellipsoid. A MADYMO seat belt was used to restrain the ATD. The seat back and pan were simulated using planes, while the cushion itself was represented by a 1-inch ellipsoid with the same properties used in figure 29. A series of simulations were conducted at various head impact angles to study the effect of this factor on the head rotation. As shown in figure 51, the ATD head rotation has an inverse relationship with the impact angle. The properties of the seat belt and seat cushion are similar to that described earlier. In figure 52, the panel is masked for better clarity of head rotation.

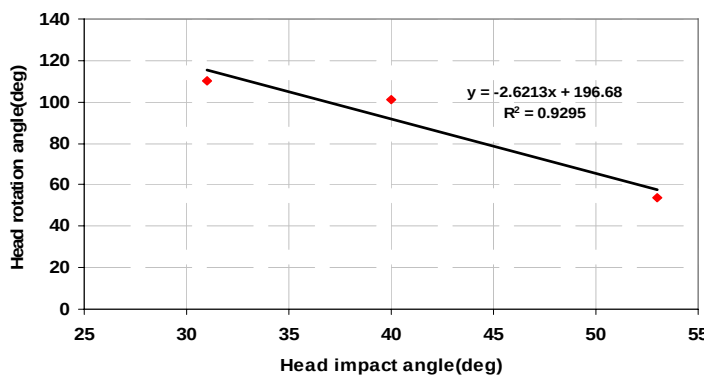

Figure 51. Head Rotation Angle and Impact Angle

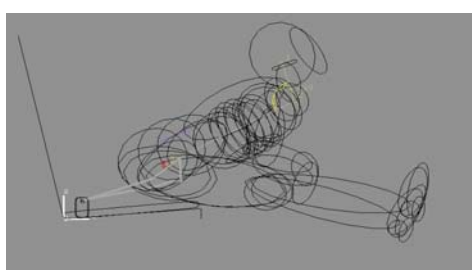

Figure 52. Head Rotation for Impact Angle of 40 Degrees

The ATD head rotates after impact, and this rotation is higher for smaller head impact angles. Therefore, it is desirable that the NHCT be modified to replicate this head rotation. This is in itself a trivial task. However, merely swapping out the neck could be problematic, since the flexible neck has proven to be unable to support the ATD head during the acceleration phase

when the actuator is firing. This requires the development of a rigid neck bracket to support the head during acceleration and then to disengage prior to impact with the target surface.

The modification and its effect on the HIC results were studied using multibody analytical tools. The rigid joint between the neck and the pendulum arm was changed to a spherical joint with the required flexion and torsional joint stiffness to emulate the ATD head kinematics when impacted on a surface with similar input parameters as depicted in figure 53. Figure 54 shows the simulation sequence for this modification.

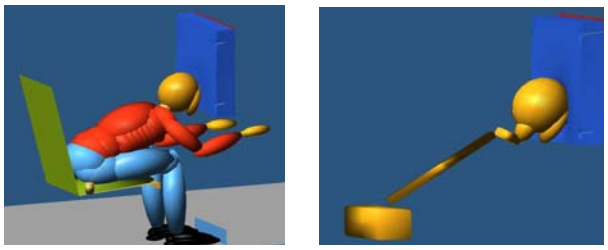

Figure 53. Head Impact for Sled Test and NHCT With Flexible Neck on Polyethylene Pad

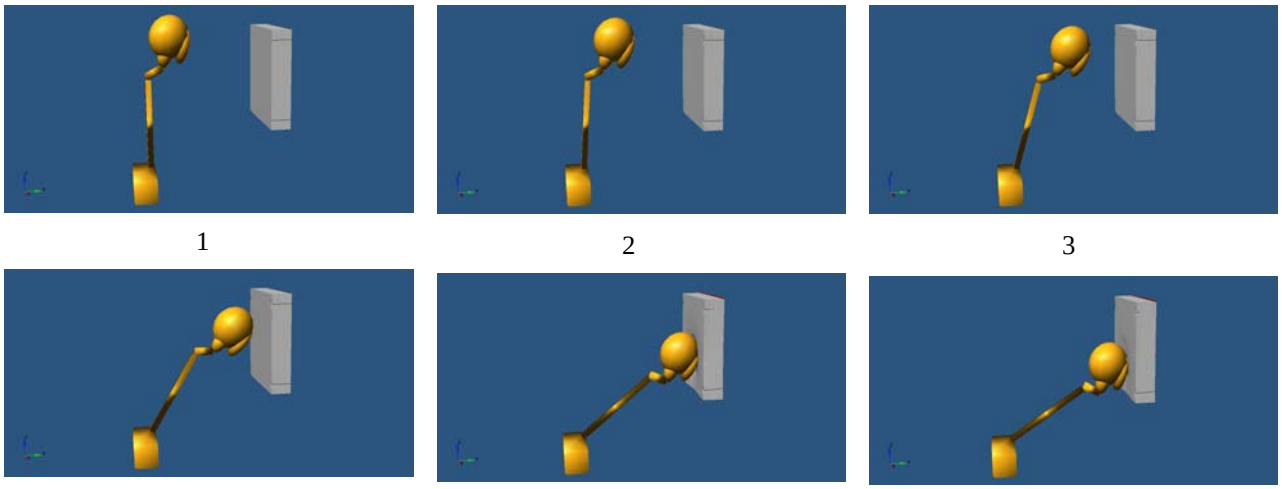

Figure 54. Simulation Sequence for NHCT With Flexible Neck

Figure 55 shows the resulting acceleration of the ATD head compared to the benchmark test. As can be seen, the NHCT model with the flexible neck has a very similar acceleration profile to the FSST test. The output is tabulated in table 16.

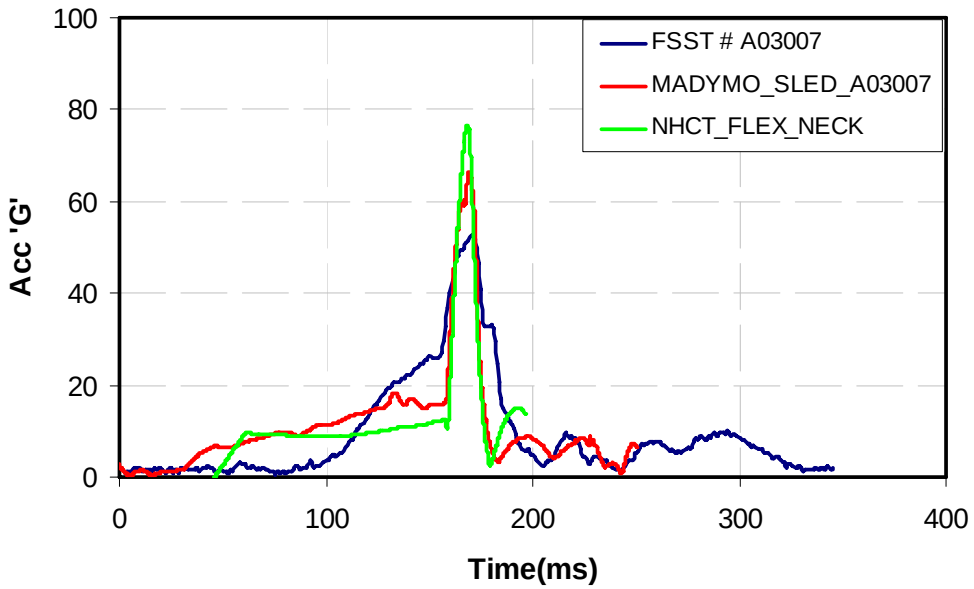

Figure 55. Comparison of Head Acceleration Profile for FSST and NHCT Model With Flexible Neck

Table 16. Comparison of Flexible and Rigid Neck NHCT Model Results and Corresponding FSST Results

Parameters	FSST A03007	MADYMO Model NHCT/Flexible-Neck H03007	MADYMO Model NHCT/Rigid-Neck H03007
Head-impact angle (deg)	45.7	45.7	45.7
Head-impact velocity(ft/sec)	32.2	32.2	32.2
HIC	304.3	347.0	440.0
HIC window (ms)	28.0	28.0	43.0
Head c.g. peak acceleration (g's)	52.0	75.0	82.0
Head c.g. avg. acceleration (g's)	33.0	36.0	42.0

Table 17 shows the results of a parametric study using the FSST and the flexible neck NHCT model. Figure 56 shows correlations between the FSST and both the rigid neck NHCT and the flexible neck NHCT models. As can be seen, the flexible neck NHCT model shows a substantially improved trend and correlation. Further tests could be carried out with various impacting surfaces and correlation drawn between rigid neck and flexible neck.

Table 17. Comparison of FSST Results With Flexible Neck NHCT Model Results

FSST				MADYMO Model of NHCT With Analytical Flexible Neck			
Test ID	Head Velocity (ft/sec)	Impact Angle (degree)	HIC	Test ID	Head Velocity (ft/sec)	Impact Angle (degree)	HIC
A03007	32.2	45.7	304	H03007	32.2	45.7	347
A03008	32.6	46.7	302	H03008	32.6	46.7	334
A03009	42.4	41.6	1047	H03009	42.4	41.6	1020
A03010	43.8	42.9	1044	H03010	43.8	42.9	920
A03011	38.7	40.6	667	H03011	38.7	40.6	870

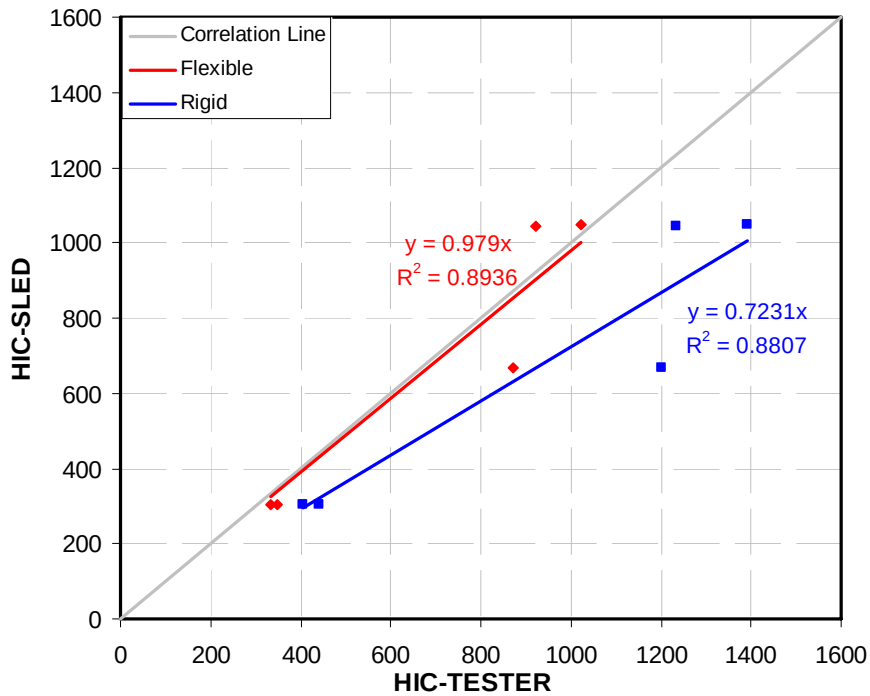

Figure 56. Correlation Between FSST and NHCT With Rigid and Flexible Necks

10. RESULTS.

This study presented a brief description of the NHCT and the latest modifications in the device. The device was aimed to produce a simple alternative method of compliance with the Head Injury Criteria (HIC) requirement for the certification of seats and interior cabin furnishings, as specified in 14 CFR 23.562 and 25.562. The performance of the device for various aircraft interior impact surfaces was compared to the performance of traditional FSST. The data was obtained from dynamic tests conducted at NIAR and CAMI as well as from occupant biodynamic models developed using MADYMO code.

In general, it appears that for simple geometries, such as panels, the NHCT device tends to produce results that are close but slightly greater than the results from FSSTs. Thus, HIC for the NHCT are conservative for the cases tested.

The effects causing descrepancies can be categorized into the following groups:

- Variations in the behavior of the test articles. These variations, such as unpredictable inertia-induced flexing of tall divider panels or different failure modes of tray tables, are unavoidable and difficult to correct.

- Variations caused by kinematic approximations in the NHCT. While the NHCT approximates a kinematic copy of the 50th percentile male Hybrid II ATD as closely as possible, some differences are present, such as lack of a flexible neck, incompressible spine, and a different lower torso friction properties. Simulations have shown that while the contribution of a flexible neck to the HIC may not be a substantial contributing factor in causing HIC values to vary from FSST values for simple target geometries, it could have a more pronounced effect for more complex targets, such as seat backs with tray tables. Designs for rectifying these limitations are available and can be implemented with relative ease.

- Variations in FSST-NHCT test conditions. As noted previously, HIC in general is extremely sensitive to test parameters, i.e., impact velocity and impact angle. This being the case, one would expect that validation of the NHCT would be difficult using a one-to-one comparison of the FSST and NHCT test data.

11. REFERENCES.

1. Chandler, R.F., "Human Injury Criteria Relative to Civil Aircraft Seat and Restraint Systems," *SAE Paper 851847, Society of Automotive Engineers*, Warrendale, PA, 1985.

2. Lissner, H.R., Lebow, M., and Evans, F.G., "Experimental Studies on the Relation Between Acceleration and Intracranial Pressure Changes in Man," *Surgery, Gynecology, and Obstetrics*, V. 111, 1960, pp 329-338.

3. Gadd, C.W., "Use of a Weighted Impulse Criterion for Estimating Injury Hazard," SAE Paper 660793, *Proceedings of the Tenth Stapp Car Crash Conference*, Society of Automotive Engineers, Warrendale, Pennsylvania, 1966, pp. 16-174.

4. Versace, J., "A Review of the Severity Index," SAE Paper 710881, *Proceedings of the Fifteenth Stapp Car Crash Conference*, Society of Automotive Engineers, Warrendale, Pennsylvania, 1971, pp. 771-796.

5. Gurdjian, E.S., Lissner, H.R., Latimer, F.R., Haddad, B.F., and Webster, J.E., "Quantitative Determination of Acceleration and Intercranial Pressure in Experimental Head Injury," *Neurology* 3,4, 1953, pp. 4223.

6. Gurdjian, E.S., Roberts, V.L. and Thomas, L.M., "Tolerance Curves of Acceleration and Intercranial Pressure and Protective Index in Experimental Head Injury," *J. of Trauma*, Vol. 6, 1964, pp. 600.

7. "Department of Transportation (1971) Occupant Crash Protection-Head Injury Criterion," NHTSA Doc Number 69-7, Notice 19, S6.2 of FMVSS 208, March 1971.

8. Title 14 Code of Federal Regulations, Part 23, Amendment 23-39, Section 23.562, published in the Federal Register, August 14, 1988.

9. Title 14 Code of Federal Regulations, Part 25, Amendment 25-64, Section 25.562, published in the Federal Register, May 17, 1988.

10. Hooper, S.J., Lankarani, H.M., and Mirza, M.C., "Parametric Study of Crashworthy Bulkhead Designs," FAA report, DOT/FAA/AR-02/103, December 2002.

11. Lankarani, H., "Development of a Component Head Injury Criteria (HIC) Tester for Aircraft Seat Certification—Phase 1," FAA report, DOT/FAA/AR-02/99, November 2002.

12. MADYMO V6.2, TNO Automotive, May 2004.

13. DeWeese, Richard L. and Moorcroft, David M., "Evaluation of a Head Injury Criteria Component Test Device" *Office of Aerospace Medicine*, Washington, DC, 20591, DOT/FAA/AM-04/18.